Pain-relieving mechanisms of vinpocetine in an animal model of chemotherapy-induced peripheral neuropathy

Nan, Guanghai

Department of Medical Science

Graduate School

Yonsei University

Pain-relieving mechanisms of vinpocetine in an animal model of chemotherapy-induced peripheral neuropathy

Advisor Lee, Bae Hwan

A Dissertation Submitted
to the Department of Medical Science
and the Committee on Graduate School
of Yonsei University in Partial Fulfillment of the
Requirements for the Degree of
Doctor of Philosophy in Medical Science

Nan, Guanghai

June 2025

Pain-relieving mechanisms of vinpocetine in an animal model of chemotherapy-induced peripheral neuropathy

This Certifies that the Dissertation of Nan, Guanghai is Approved

Committee Chair	Lee, Jong Eun
Committee Member	Lee, Bae Hwan
Committee Member	Shim, Insop
Committee Member	Jung, Hyun Ho
Committee Member	Kim, Hee Young

Department of Medical Science
Graduate School
Yonsei University
June 2025

ACKNOWLEDGEMENTS

Four and a half years have flown by in the blink of an eye. Looking back, this journey has been filled with challenges, discoveries, and growth, transforming me from someone who knows almost nothing to someone who now grasps the fundamentals of the field. This transformation would not have been possible without the support, guidance, and companionship of many individuals to whom I am deeply grateful.

First and foremost, I would like to express my sincere gratitude to my advisor, Professor Bae Hwan Lee**,** for his patience, wisdom, and unwavering support. His insightful guidance has shaped not only my research but also my ability to think critically and independently. His encouragement at every stage gave me confidence to push forward, even in the face of difficulties.

I am profoundly grateful to Professor Jong Eun Lee, Professor Insop Shim, Professor Hyun Ho Jung, and Professor Hee Young Kim for their invaluable guidance and support throughout my dissertation process, from providing expert advice to serving as members of the review committee. Their insightful feedback helped me identify the shortcomings of my research, refine my experiments, and improve the quality of my dissertation.

I sincerely appreciate Assistant Professor Myeounghoon Cha, who introduced me to this field and guided me during the initial stages of my research. His mentorship laid the foundation for my understanding and helped me navigate the complexities of the subject. I also extend my sincere appreciation to Professor Hee Young Kim, whose expertise in experimental design contributed significantly to the structure and success of this research. Their valuable insights and meticulous guidance helped refine my approach and achieve meaningful results.

I would like to thank Teaching Assistant Un Jeng Kim, whose technical expertise and unwavering support were instrumental in the success of my experiments. Beyond her professional guidance, her companionship during this journey made even the toughest days bearable. I am also deeply grateful to Professor Kyung Hee Lee, the first mentee of our professor, whose regular visits to the laboratory and insightful advice have been inspiring and motivating. Additionally, I sincerely thank Professor Minjee Kwon, whose encouraging words during her visits over school breaks always lifted my spirit and reminded me to keep going.

I am also deeply grateful for the companionship of my laboratory colleagues, who enriched this journey and made it memorable. Kyeongmin Kim, whose experience and advice guided me when everything felt overwhelming; Leejeong Kim, my peer, with whom I shared countless discussions, struggles, and moments of discovery; and Lin Lin and Nari Kang, my juniors, who reminded me that learning is a continuous process and that curiosity is a driving force. Through long hours in the laboratory, shared frustrations, and small victories, their presence made this experience truly special.

My heartfelt thanks to my family, who stood by me through every high and low. Their unwavering belief in me, patience, and endless support have been my greatest source of strength. Even from a distance, their encouragement always reached me at the right moment, reminding me of the reasons I embarked on this path.

Four and a half years ago, I took my first steps into this field with uncertainty. Today, as I reach this milestone, I realize that this journey has been about more than just gaining knowledge—it has been about resilience, growth, and the incredible people who have walked this path with me. To each and every one of you, I extend my deepest gratitude.

Guanghai Nan
June 2025

TABLE OF CONTENTS

LIST OF FIGURES

ABSTRACT

Pain-relieving mechanisms of vinpocetine in an animal model of chemotherapy-induced peripheral neuropathy

Chemotherapy-induced peripheral neuropathy (CIPN) is a major dose-limiting side effect of cancer treatment, characterized by sensory disturbances, chronic pain, and motor dysfunction. Despite its high prevalence, effective treatment options remain limited due to the complex and multifactorial nature of CIPN pathophysiology. Among the key contributors, oxidative stress and mitochondrial dysfunction play critical roles in neuronal damage and pain sensitization. Increased reactive oxygen species (ROS) production, mitochondrial dysfunction, and impaired antioxidant defense contribute to CIPN development, making mitochondria a promising therapeutic target for CIPN. Vinpocetine, a synthetic derivative of vincamine, exhibits neuroprotective effects, including antioxidant, anti-inflammatory, and mitochondrial-enhancing properties. While widely used in neurological disorders, such as stroke and dementia, the role of vinpocetine in CIPN remains unclear. This study aimed to evaluate the analgesic effects and underlying mechanisms of vinpocetine in a CIPN model.

Mice were treated with paclitaxel to induce CIPN and received either single or repeated vinpocetine administration. Behavioral tests were conducted to assess mechanical, thermal, and cold hypersensitivity. Western blot analysis was performed to examine mitochondrial function via the PGC-1α/NRF1/TFAM pathway and SOD2 expression. Furthermore, ROS levels were examined by MitoSOX staining. Voltage-sensitive dye imaging (VSDI) was used to evaluate neuronal activity in the spinal cord, while Western blot was used to examine changes in the expression of AMPA, NMDA receptors (NR2A and NR2B), and associated kinases (PKC-α, CaMKII-α, and PKA). Furthermore, immunohistochemistry was performed to evaluate the intensity of AMPA and PKC-α expression in the spinal cord dorsal horn, as well as their colocalization with NeuN.

The results demonstrated that vinpocetine effectively reduced oxidative stress-induced pain. Administration of vinpocetine at a dose of 20 mg/kg significantly alleviated pain symptoms, with repeated treatment producing cumulative analgesic effects. Vinpocetine exhibited antinociceptive effects at the spinal cord level during both the early and late stages of CIPN. Repeated vinpocetine treatment reduced mitochondrial ROS levels, upregulated the PGC-1α/NRF1/TFAM signaling pathway, and restored SOD2 expression.

VSDI results identified the stimulation threshold in the CIPN model as 0.3 mA. Additionally, VSDI analysis confirmed a reduction in neuronal hyperexcitability following vinpocetine treatment, with the effect lasting for more than two hours. Downregulation of AMPA and NR2B receptors, along with PKC-α inhibition, suggested a reduction in central sensitization. Furthermore, immunohistochemistry revealed a decrease in the intensity of AMPA and PKC-α expression, as well as reduced colocalization with NeuN-positive neurons.

These findings highlight vinpocetine as a promising therapeutic candidate for CIPN, which acts through mitochondrial protection and modulation of central sensitization. By restoring mitochondrial homeostasis, reducing oxidative stress, and regulating neuronal excitability, vinpocetine could be used as a potential strategy for CIPN management.

Key words: chemotherapy-induced peripheral neuropathy, vinpocetine, mitochondrial biogenesis, oxidative stress, neuronal hyperexcitability, central sensitization.

1. Introduction

Chemotherapy-induced peripheral neuropathy (CIPN) is a common and often debilitating adverse effect of chemotherapeutic agents, such as platinum-based drugs, taxanes, and vinca alkaloids.[1,2] While acute CIPN symptoms may resolve after chemotherapy cessation, evidence suggests that approximately 68% of patients develop CIPN within the first month, with 30% experiencing symptoms persisting over six months.[3] Patients with CIPN present neuropathic symptoms ranging from tingling, burning sensations, and numbness to severe chronic pain and motor dysfunction.[4,5] These symptoms are commonly distributed distally, bilaterally and symmetrically, resembling a "glove-and-stocking" pattern.[4] Besides its clinical burden, CIPN has a significant socioeconomic impact, often necessitating dose reductions or even discontinuation of chemotherapy, thereby compromising treatment efficacy and negatively affecting patient survival outcomes.[6-8] Despite its clinical significance, effective treatment options remain limited, posing a major challenge in oncology and supportive care.[9,10]

Over the past decades, many hypotheses about the mechanisms of CIPN have been proposed, involving oxidative stress, apoptotic processes, disrupted calcium homeostasis, axonal degeneration, membrane remodeling, and neuroinflammation.[11] Although several chemicals suppressing these pathological changes have been developed for symptomatic relief of CIPN, they often lack efficacy and/or have unacceptable side-effect.[12] Currently, only duloxetine is recommended for the treatment of CIPN, with limited efficacy[13] Therefore, it remains essential to explore more effective therapeutic approaches to alleviate symptoms and prevent neuropathy.

Considerable alterations in the structural integrity and functionality of mitochondria are found in CIPN models and influence the onset, progression, and severity of CIPN.[14] Most chemotherapeutics induce damage to both neuronal and non-neuronal mitochondria, which are responsible for producing roughly 90% of cellular reactive oxygen species (ROS).[15] The disparity between mitochondrial ROS production and elimination, caused by excessive ROS generation and diminished antioxidant defense activity, leads to oxidative stress, which is pivotal in brain injury and chronic pain.[16] Research indicates that the overproduction of ROS results in oxidative damage to proteins, lipids, and DNA, subsequently inducing apoptosis and neuroinflammation.[17,18] These processes may inflict secondary damage on mitochondria, exacerbating the generation of ROS and the pathogenic mechanisms of oxidative stress.[11] Mitochondrial dysfunction is a major consequence of oxidative stress, resulting in impaired ATP production, increased neuronal excitability, and chronic pain. It has been reported that ROS scavengers such as N-tert-

butyl-α-phenylnitrone (PBN), 4-hydroxy-2,2,6,6-tetramethylpiperidine-1-oxyl (TEMPOL), and various antioxidants effectively attenuate pain symptoms in CIPN models,[19,20,21-23] suggesting a critical role of mitochondrial ROS in pain generation.

In paclitaxel-induced neuropathy models, in which paclitaxel, a taxane-based chemotherapeutic agent, is used, swollen and vacuolated mitochondria are observed in both myelinated and unmyelinated sensory neurons, reinforcing the association between mitochondrial damage and CIPN.[24] Proliferator-activated receptor coactivator-1α (PGC-1α) is a transcriptional coactivator of mitochondrial biogenesis, antioxidant enzyme expression,[25] and regulates mitochondrial mass, facilitating tissue adaption to increased energy demands.[26,27] The balance between ROS production and antioxidant defense mechanisms can be disrupted when mitochondrial biogenesis is altered.[28] CIPN animal models revealed the downregulation of PGC-1α-mediated mitochondrial biogenesis genes, indicating its crucial role in CIPN development.[29] As PGC-1α modulates antioxidant enzymes such as superoxide dismutase 2 (SOD2) and uncoupling protein 2 (UCP2),[25] recovery of PGC-1α in CIPN models may alleviate CIPN pain symptoms by normalizing mitochondrial function and antioxidant defense.

It is well accepted that chemotherapeutic agents penetrate dorsal root ganglion (DRG) well and alter ion channel expression, increase inflammation, and cause neuronal hyperexcitability in neurons.[30-32] As well as DRG in the development of CIPN, the spinal cord dorsal horn is also critically involved in processing and amplifying pain signals of CIPN.[33] When spinal dorsal horn neurons are subjected to central sensitization, they exhibit increased excitability and synaptic transmission and amplify pain perception.[34] Central sensitization is caused by activation of AMPA receptors, NMDA receptor subunits (NR2A/NR2B), and intracellular signaling pathways such as PKA, PKC, and CaMKII.[35] As signaling molecules involved in spinal central sensitization, ROS increased the levels of activated protein kinases, phosphorylation of AMPA and NMDA receptors and excitability of spinal dorsal horn neurons,[36] and lead to persistent pain.[15] In particular, mitochondria-derived ROS play an important role in persistent pain. Mitochondria-targeted ROS scavengers like triphenylphosphonium chloride (MitoTEMPO) effectively reduce excitatory synaptic strength and neuropathic mechanical hypersensitivity,[37] and overexpression of mitochondrial SOD in spinal dorsal horns suppresses capsaicin-induced secondary hyperalgesia in mice.[38] Lowering mitochondrial ROS may reduce pain symptoms in CIPN models.[39]

Vinpocetine, a dietary supplement derived from the alkaloid vincamine, has antioxidant and anti-inflammatory properties and is used to improve brain function in the patients with stroke, dementia, and neurodegenerative diseases.[40,41,42,43] While vinpocetine has not been widely evaluated in preclinical models of pain, some studies have shown its potential

analgesic effects. For example, vinpocetine inhibited inflammatory cytokines and NF-κB activation, and reduced acute inflammatory pain-associated behaviors.[43,44] Vinpocetine reduced thermal nociception and abdominal constriction in a mouse model of visceral pain.[45] To date, the analgesic effects on CIPN have not been explored. Given its antioxidant effect, well-established safety profiles, and long history of clinical use,[41] vinpocetine may be a promising candidate for CIPN treatment.

Thus, this study aimed to investigate the pain-relieving mechanisms of vinpocetine at the spinal cord level in a CIPN model. Specifically, this study investigated whether vinpocetine (1) produces pain-relieving effects in a CIPN model, (2) restores mitochondrial biogenesis and antioxidant enzyme through the PGC-1α pathway, (3) reduces oxidative stress and central sensitization in the spinal dorsal horn, and (4) modulates CIPN-associated intracellular signaling.

2. Materials and methods

2.1. Experimental animals

Adult male C57BL/6 mice (6 weeks; 20-22 g; Orient Bio, Sungnam, Gyonggi, Korea) were used. Mice were housed in groups of five with sawdust bedding, in a climate-controlled environment with 12-hour light/dark cycle. Laboratory diet was available *ad libitum*, except when the mice were being tested. Animals were allowed to acclimate for at least 7 days after arrival at the Association for Assessment and Accreditation of Laboratory Animal Care (AAALAC)-accredited Yonsei University College of Medicine Animal Care Facilities. All animal procedures adhered to the National Institutes of Health guidelines and were approved by the Institutional Animal Care and Use Committee of Yonsei University Health System (permit no.: 2023-0010).

2.2. Experimental design

The present study was designed to investigate the pain-relieving effects of vinpocetine on CIPN. The specific objectives were as follows:

(1) Effect of acute treatment of vinpocetine on CIPN: To investigate the analgesic effects of vinpocetine in CIPN, an intraperitoneal injection of vinpocetine was given in the CIPN mice. Mechanical hypersensitivity was assessed using the von Frey filament test (Figure 1a).

(2) Effect of repeated treatments of vinpocetine on CIPN: To investigate the effects of daily treatment of vinpocetine on CIPN, vinpocetine was injected intraperitoneally once daily from 7 (PID7) up to 13 days (PID13) after the first injection of paclitaxel. Mechanical, thermal, and cold hypersensitivities were measured before (Pre) and on PID3, PID7, PID9, PID11, PID13, and PID14 after paclitaxel administration (Figure 1b).

(3) Effect of vinpocetine on superoxide-mediated pain: To explore the mediation of ROS in the effect of vinpocetine on CIPN, the effects of vinpocetine on intrathecal antimycin A and potassium superoxide-induced pain were evaluated using the von Frey filament test.

(4) The effects of vinpocetine on chemotherapy-induced molecular changes in the spinal dorsal horn: To examine whether repeated vinpocetine treatment can restore the molecular changes in the spinal dorsal horn in the CIPN model, CIPN mice received

daily intraperitoneal injections of vinpocetine. On PID14, after the completion of the behavioral test (2 hours after the last injection of vinpocetine), the spinal cords were taken out, and the levels of ROS, Western blot, and immunohistochemistry (IHC) were examined in the spinal dorsal horn of CIPN mice (Figure 1c).

(5) The effect of vinpocetine on the neuronal excitability of the spinal dorsal horn in the CIPN model: *in vitro* voltage-sensitive dye imaging (VSDI) was performed on the spinal dorsal horn isolated from CIPN mice on PID14. Spinal cord slices were exposed to bath application of either vinpocetine or vehicle (DMSO) (Figure 1d).

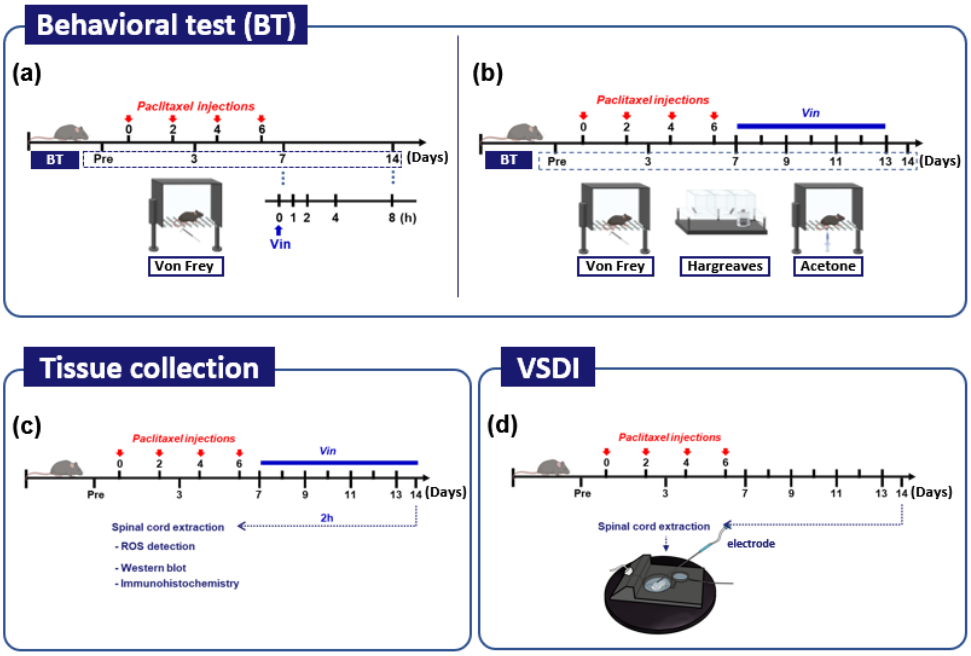

Figure 1. Overall experimental design illustration. (a, b) Behavioral test: Effect of single (a) or repeated (b) treatment of vinpocetine on pain behaviors in CIPN mice. Paclitaxel was administered on PID 0, 2, 4, and 6. Mechanical sensitivity following paclitaxel injections was measured on Pre (before paclitaxel) and PID3, PID7, and PID14. The effect of single treatment of vinpocetine was assessed by von Frey filament test on PID7 and PID14 (a). The effect of repeated vinpocetine application was assessed by von Frey filament test, Hargreaves test, and acetone test on PID7, PID9, PID11, PID13, and PID14 (b). (c) ROS detection, Western blot and immunohistochemistry: On PID14, the spinal cords from paclitaxel-treated mice were collected 2 hours after vinpocetine treatment and processed. (d) Voltage-sensitive dye imaging (VSDI): Real-time VSDI for neuronal activation of the spinal dorsal horn neurons was performed on PID14 in paclitaxel-treated mice.

2.3. Chemotherapy-induced peripheral neuropathy (CIPN) model

CIPN was induced using paclitaxel as described previously.[46] In brief, paclitaxel (T7402; Sigma-Aldrich, St. Louis, MO, USA) was prepared at 25 mg/ml in a mixture of 50% Cremophor® EL and 50% anhydrous ethanol, and kept in a deep freezer until use. The stock solution was diluted with 0.9% sterile saline immediately before injection. The mice received 4 intraperitoneal (i.p.) injections of paclitaxel on four alternate days (days 0, 2, 4, and 6) at a dose of 2 mg/kg per injection.

2.4. Drug administration

Intrathecal injection (i.t.) injection in mice was performed as described previously.[47] Briefly, under isoflurane anesthesia (Hana Pharm, Songnam, Gyeonggi, Korea), the hair on back was shaved. A 31-gauge needle attached to a 50 μl Hamilton syringe was slowly introduced into lumbar 5 (L5) and L6. When mice revealed an abrupt tail flick response to the needle, drugs such as vinpocetine, antimycin A, and potassium superoxide were then slowly injected into the spinal cavity. The location of the intrathecal injection was further confirmed using an X-ray imaging system (NR-F100, NanoRay Inc., Hsinchu, Taiwan). After confirmation, the needle was held in place for 1 minute before withdrawal to prevent reflux of the injected solution.

Vinpocetine (V6383, Sigma-Aldrich) was dissolved using a vehicle of 5% dimethyl sulfoxide (DMSO) in saline prior to administration. Vinpocetine was prepared at different dosages of 2.5 mg/kg, 5 mg/kg, 10 mg/kg, and 20 mg/kg for i.p. injection and a dose of 20 μg/kg in a volume of 10 μl for i.t. injection. Antimycin A (A8674, Sigma-Aldrich) was dissolved in 1× phosphate-buffered saline (PBS) containing 1% DMSO to a final concentration of 50 μM and administered i.t. in a volume of 10 μl. The control group received an equivalent volume of vehicle (1% DMSO in PBS) to match the experimental conditions. Potassium superoxide (355420250, Thermo Scientific Chemicals, Waltham, MA, USA) was prepared at a 100 mM concentration in PBS, and 5 μl was administered intrathecally. The control group received an equivalent volume of vehicle. All injections were performed under strict aseptic conditions, and the mice were monitored post-injection for signs of distress or adverse reactions.

2.5. Behavioral assessment

Pain behaviors in mice were assessed as described in a previous study.[33] All behavioral tests were conducted in a blinded manner.

Mechanical hypersensitivity was assessed using the up-down method with a set of calibrated von Frey filaments (0.02, 0.04, 0.07, 0.16, 0.4, 0.6, 1.0, and 1.4 g; Stoelting, Chicago, IL, USA).[48] Each mouse was habituated on a wire mesh floor in a transparent plastic box for at least 30 minutes prior to test. Each filament was placed on the plantar surface to bend slightly for a few seconds. Withdrawal or tremor of the hindpaw during stimulation or shortly following the removal of the stimulus was considered positive. The initial stimulus commenced with the 0.4 g filament. In the event of a favorable reaction, a less robust filament was utilized. Subsequent to the initial alteration in responses, four further responses were recorded, and the 50% mechanical withdrawal threshold (MWT) value was determined.

Thermal hypersensitivity was assessed using the Hargreaves test with a plantar test device (7371 plantar test; UgoBasile, Milano, Italy). Mice were allowed to move freely within an open-topped transparent plastic cylinder (6 cm diameter × 16 cm height) on a glass floor for 20 minutes before the test. A mobile radiant heat source was then placed under the glass floor and focused on the hindpaw. The infrared (IR) intensity was set at 50%, which is considered optimal for preventing tissue damage while eliciting paw withdrawal latency (PWL). PWLs were measured with a cut-off time of 20 seconds. Heat stimulation was repeated five times with a 10-minute interval to obtain the mean latency of paw withdrawal.

Cold hypersensitivity was assessed by observing foot withdrawal responses (lifting, shaking, or licking) following the application of cold stimuli to the plantar surface of the paw. A drop of 100% acetone was delicately applied to the left hind paw of the mice using a 1 cc syringe connected to a PE10 tube. The test was repeated five times with an interval of approximately 3 to 5 minutes between each repetition. The response frequency to acetone was expressed as a percentage response frequency.

2.6. Estimation of mitochondrial ROS levels in the spinal dorsal horn

MitoSOX Red (M36008, Invitrogen, Carlsbad, CA, USA) was dissolved in DMSO to create a 5 mM stock solution and then diluted with 0.9% sterile saline to a final concentration of 33 μM. On PID 14, 10 μl of MitoSOX Red was injected i.t. under isoflurane anesthesia using a direct transcutaneous approach in mice. Approximately 5-6

hours after MitoSOX Red injection, L4-6 spinal cord segments were removed and post-fixed in 4% paraformaldehyde (PFA) overnight at 4 °C. The spinal cords were kept in a 30% sucrose solution for 2 days, cryosectioned at 20 μm thickness and then mounted on gelatin-coated slides. The sections were washed with 1× PBS for 10 minutes, three times, and coverslipped with mounting medium (H-1000, Vector Laboratories, Burlingame, CA, USA). The specimens were analyzed using a fluorescence microscope equipped with a rhodamine filter. Laminae III-V of the dorsal horn were imaged from 10 randomly chosen sections per mouse using an LSM710 (Carl Zeiss, Jena, Germany) microscope with a 63× oil immersion objective lens. The MitoSOX Red-positive cellular profiles exhibiting unique nuclei (black oval-shaped regions encircled by red granules) were quantified as described previously.[38]

2.7. Western blot analysis

On PID14 after the last injection of vinpocetine, L4-6 spinal cord segments were harvested, promptly frozen in liquid nitrogen, and preserved at -70 °C for subsequent analyses. The tissues were homogenized using a combination of lysis buffer (PRO-PREP; Intron Biotechnology, Pyeongtaek, Korea) and a protease inhibitor cocktail (P8340; Sigma-Aldrich), followed by centrifugation at 15,000 rpm for 10 minutes. The supernatants containing the proteins were transferred into a sterile tube. The protein concentration was quantified using a BCA kit. Total protein (20 μg) was prepared and loaded into an 8%-10% acrylamide gel, and then transferred onto a PVDF transfer membrane (Merck Millipore, Darmstadt, Germany). The membranes were incubated with 5% skim milk (SM2010; GeorgiaChem, Norcross, GA, USA) for 1h at room temperature (RT), followed by overnight incubation with the primary antibody overnight at 4 °C. The primary antibodies used were PGC-1α (1:1000, PA5-72948, Thermo Fisher Scientific, Waltham, MA, USA), NRF-1 (1:1000, no. 46743, Cell Signaling Technology, Beverly, MA, USA), TFAM (1:3000, NBP2-19437, Novusbio, CO, USA), anti-SOD2 (1:5000, ab13533, Abcam, Cambridge, UK), AMPA (1:5000, ab183797, Abcam), NR2A (1:1000, ab124913, Abcam), NR2B (1:2500, ab65783, Abcam), PKC-α (1:5000, ab11723, Abcam), CaMKII-α (1:5000, ab52476, Abcam), and PKA (1:5000, ab75991, Abcam). GAPDH (1:10000, LF-PA0018, ABFrontier, Seoul, Korea) was used as an internal loading control. The membrane was subsequently incubated with a secondary anti-rabbit antibody (1:5000; no. 7074, CST) for 2 hours at RT. The antibody-labeled protein bands were imaged with an enhanced chemiluminescence reagent (ECL; RPN2232, Cytiva, Marlborough, MA, USA) and Cytiva (IQ800), and the intensities were quantified using Image J.

2.8. Immunohistochemistry

On PID14, after the last treatment with vinpocetine, the animals were anesthetized with sodium pentobarbital (50 mg/kg, i.p.) and subsequently perfused transcardially with 0.9% sterile normal saline, followed by 4% PFA (pH 7.4) for tissue fixation. The L4-L5 spinal cords were isolated and post-fixed overnight at 4 °C in a 4% PFA solution. The tissues were then cryoprotected by immersion in 30% sucrose in 1× PBS for 24 hours at 4 °C, imbedded in O.C.T. compound, swiftly frozen in liquid nitrogen, and preserved at -70 °C for further processing. The spinal cord segments were transversely sliced to a thickness of 20 μm using a cryostat and affixed to glass slides for immunohistochemical staining. Before staining, the slides containing sectioned tissues were treated in 10 mM sodium citrate buffer (pH 6.0) at 95 °C for 10 minutes to promote antigen retrieval. After cooling to RT, the sections were washed three times with 1× PBS (5 minutes each) and then incubated in 0.3% PBST (1× PBS containing 0.3% Triton X-100) for 15 min to enhance permeability. To minimize nonspecific binding, the sections were incubated with a blocking solution (10% normal donkey serum in 0.3% PBST) for 1 hour at RT. They were then incubated overnight at 4 °C with primary antibodies diluted in the blocking solution. The primary antibodies used were Anti-Glutamate Receptor 1 (GluR1, AMPA subtype) antibody [EPR19522] (1:200, ab183797, Abcam), NeuN (1:1000, ab104222, Abcam), and PKC-α (1:500, A302-446A, Thermo Fisher Scientific). Following primary antibody incubation, the sections were washed three times with 0.3% PBST (5 minutes each) and then incubated with the appropriate fluorescently labeled secondary antibodies for 2 hours at RT in the dark. After secondary antibody incubation, the sections were washed again with 0.3% PBST (three times, 5 minutes each). For nuclear counterstaining, the sections were incubated with DAPI (H-1200, Vector Laboratories). Coverslips were applied to the pieces and sealed to avert desiccation. Fluorescent images were obtained under a Zeiss LSM 700 laser scanning confocal microscope (Carl Zeiss, Jena, Germany) at 20× magnification (0.5× zoom) and 40× magnification (0.5× and 1.0× zoom). Representative images were processed via maximum intensity projection (MIP) and exported using Zen Black software (Carl Zeiss). The stained area and mean fluorescence intensity (MFI) of the MIP images were quantified using the Zen Blue software (Carl Zeiss) and ImageJ (NIH, Bethesda, MD, USA). Fluorescence intensity levels were standardized and statistically analyzed.

2.9. Voltage-sensitive dye imaging (VSDI)

On PID 14 (Figure 1d), the mice were deeply anesthetized with urethane (1.25 g/kg, i.p.)

and transcardially perfused with ice-cold solution containing 213 mM sucrose, 2.5 mM KCl, 1.25 mM NaH_2PO_4, 10 mM $MgSO_4$, 0.5 mM $CaCl_2$, 26 mM $NaHCO_3$, and 11 mM glucose. The spinal cord including L4-L5 was carefully taken out and rapidly cooled in ice-cold solution for 5 minutes. Excess water was removed from the surface using filter paper, and glue was applied to the concave edge of an agarose block. The spinal cord was gently placed on the glued edge, and the L2 and L5 ends were trimmed using razor blades. An agarose block was mounted upright on the specimen plate. The specimen plate was placed in a vibratome buffer tray filled with an ice-cold solution. Transverse spinal cord sections of 400 μm were obtained using a vibratome (Leica Biosystems Inc., Buffalo Grove, IL, USA). The sections were immediately transferred to interface chambers filled with oxygenated artificial cerebrospinal fluid (aCSF), consisting of 126 mM NaCl, 2.5 mM KCl, 1.25 mM NaH_2PO_4, 2 mM $MgCl_2$, 2 mM $CaCl_2$, 26 mM $NaHCO_3$, and 10 mM glucose, saturated with 95% O_2 and 5% CO_2 (pH 7.2). Following 1 hour of recovery at RT in flowing aCSF, the sections were stained for 1 hour with a voltage-sensitive dye (VSD; di-2-ANEPEQ, 50 μg/mL in saline; Molecular Probes, Eugene, OR, USA).

For optical imaging, a concentric bipolar microelectrode (30213, FHC, Bowdoin, ME, USA) was carefully inserted into the region of interest (ROI) under an optical microscope (Olympus Optical Co. Ltd., Tokyo, Japan) outfitted with a 10× objective and 0.35× projection lens, situated above the recording site. Electrical stimulation was administered in the form of square pulses (width: 2 ms, interstimulus interval: 5 s, intensity adjusted to evoke responses) using a stimulus isolation unit (World Precision Instruments, Sarasota, FL, USA). Neuronal signals were captured using an optical imaging system featuring a high-resolution CCD camera (Brainvision Inc., Tokyo, Japan), which included a dichroic mirror, 510–555 nm excitation filter, and 590 nm absorption filter. A 150 W tungsten-halogen lamp was used as the fluorescence source. The imaging region comprised 184 × 124 pixels.

The fluorescence intensity was measured for 943.5 ms throughout each experiment. Optical signals were obtained with an optical imaging recording device (MiCAM02, Brainvision Inc.) at a frame rate of 3.7 ms per frame, with signals averaged across 20 iterations. To standardize the fluorescence intensity among pixels, the intensity change (ΔF) in each pixel was represented as a fractional change compared to the original fluorescence intensity (F), ΔF/F. The amplitudes of optical signals and the dimensions of the activated regions were ascertained utilizing a spatial filter (9 × 9 pixels) and a cubic filter (3 × 3 pixels). Data collection and analysis were conducted using the BV Analyzer software (Brainvision Inc.). Optical signals were measured as %ΔF/F, indicating the fractional fluorescence change inside a region of interest (ROI) with a radius of 2 in the dorsal horn of the spinal cord. A systematic analysis was conducted on variations in the optical intensity

and activation area.

2.10. Statistical analysis

Statistical analyses were performed using GraphPad Prism 10.1.0 (GraphPad Software, San Diego, CA, USA). The behavioral test data for von Frey filament test, Hargreaves test and acetone test were analyzed using a two-way analysis of variance (ANOVA) with repeated measures (RM), followed by Bonferroni's test for post hoc comparisons. Western blot and IHC data were analyzed by one-way ANOVA followed by Tukey's test for multiple comparisons. Differences in the intensities of optical signals and areas of activation were analyzed using paired t-test and two-way ANOVA, followed by Bonferroni's test for post hoc comparisons. All values are presented as means ± standard error of the mean (SEM). P values less than 0.05 were considered statistically significant.

3. Results

3.1. A systemic administration of vinpocetine alleviates mechanical hypersensitivity in CIPN model

Mice received i.p. injections of paclitaxel (PTX, 2 mg/kg) every other day, for a total of four injections, beginning on day 0. The von Frey test was conducted before injection (Pre), post-injection days 3 (PID3), PID7, and PID14. On PID7 and PID14, vinpocetine was administered at various dosages after the pre-behavioral test (denoted as 0 h), and the von Frey test was performed at 1-, 2-, 4-, 8-, and 12-hours post-administration (Figure 2a). The 50% MWT of PTX-treated mice showed a significant decrease on PID3, with further reductions observed on PID7 and persisting through PID14 (Figure 2b; Pre: $p < 0.001$; PID3: $p < 0.001$; PID7: $p < 0.001$; PID14: $p < 0.001$ for days: $F_{3, 108} = 417.0$, $p < 0.001$; for groups: $F_{5, 36} = 62.53$, $p < 0.001$; for days × groups: $F_{15, 108} = 19.79$, two-way ANOVA with RM followed by Bonferroni's multiple comparison test), indicating the establishment of the CIPN model.

To evaluate the analgesic effects of vinpocetine on CIPN, doses of 2.5, 5, 10, or 20 mg/kg were administered i.p. to PTX-treated mice on PID7 (Figure 2c). At the 1-hour (h) timepoint, mice treated with 5, 10, and 20 mg/kg vinpocetine displayed higher 50% MWTs than those in the vehicle-treated (PTX-Veh) group, in a dose-dependent manner (5 mg/kg: $p < 0.05$; 10 mg/kg: $p < 0.01$; 20 mg/kg: $p < 0.001$; for time: $F_{5, 180} = 19.82$, $p < 0.001$; for groups: $F_{5, 36} = 101.2$, $p < 0.001$; for time × groups: $F_{25, 180} = 5.029$, $p < 0.001$, two-way ANOVA with RM followed by Bonferroni's multiple comparison test). By the 2 h point, the 50% MWTs in the 5, 10, and 20 mg/kg groups were significantly elevated compared to those in the PTX-Veh group, with the 20 mg/kg dose showing greater efficacy than the 10 mg/kg dose (5 mg/kg: $p < 0.01$; 10 mg/kg: $p < 0.001$; 20 mg/kg: $p < 0.001$, two-way ANOVA RM followed by Bonferroni's multiple comparison test). These effects slowly returned to the baseline level over 8 hours after injection. To further confirm the analgesic effect of vinpocetine during the maintenance phase of CIPN, the behavioral tests repeated on PID14 (Figure 2d). At the 1, 2, and 4 h timepoints, the 10 and 20 mg/kg groups showed significant increases in MWTs relative to the PTX-Veh group (In 10 mg/kg, 1 h: $p < 0.01$, 2 h: $p < 0.001$; 4 h: $p < 0.05$; In 20 mg/kg, 1 h: $p < 0.001$, 2 h: $p < 0.001$; 4 h: 0.01; for time: $F_{5, 180} = 31.64$, $p < 0.001$; for groups: $F_{5, 36} = 85.03$, $p < 0.001$; for time × groups: $F_{25, 180} = 2.584$, $p < 0.001$, two-way ANOVA with RM followed by Bonferroni's multiple comparison test), with peak values observed at the 2 h mark. Notably, the 10 mg/kg and 20 mg/kg doses produced the analgesic effects of similar peak MWT levels. By the 8 and 12

h timepoints, 50% MWTs in all vinpocetine-treated groups had returned to baseline levels comparable to the PTX-Veh group. Collectively, the results indicate that vinpocetine attenuated mechanical hypersensitivity in a mouse model of CIPN and produced a profound effect at 20 mg/kg.

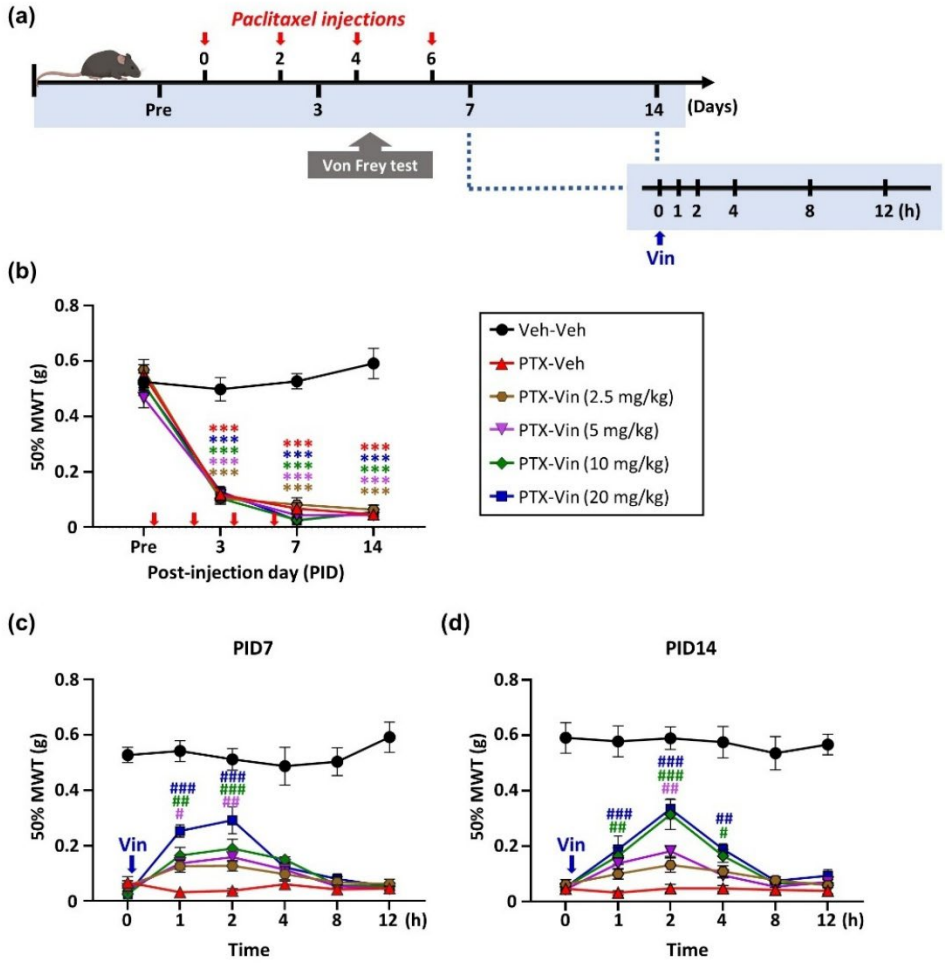

Figure 2. Effects of systemic vinpocetine treatment on mechanical sensitivity in a mouse model of CIPN. (a) An illustration of experimental timeline for drug administration and behavioral test. The von Frey filament test was performed at baseline (Pre) and on days 3, 7, and 14. Additionally, behavioral tests were conducted at 7- and 14-day time points. (b) Development of mechanical hypersensitivity following repeated PTX injections. Red arrows indicate PTX injections. The PTX

groups [PTX-Veh, PTX-Vin (2.5 mg/kg), PTX-Vin (5 mg/kg), PTX-Vin (10 mg/kg), PTX-Vin (20 mg/kg)] exhibited a significant reduction in 50% MWT from PID3 to PID14 ($p < 0.001$, n = 7 per group). (c-d) The analgesic effect of vinpocetine on mechanical hypersensitivity. The blue arrow indicates vinpocetine administration. (c) A profound antinociceptive response was observed in the PTX-Vin (20 mg/kg) group, particularly 2 hours after injection on PID7 compared to the PTX-Veh group. (d) On PID14, both PTX-Vin (10 mg/kg) and PTX-Vin (20 mg/kg) showed the most significant analgesic effect at the 2 h point ($p < 0.001$, n = 7 per group). Data are presented as mean ± SEM. $^{***}P < 0.001$ vs. Veh-Veh group, $^{\#}p < 0.05$, $^{\#\#}p < 0.01$, and $^{\#\#\#}p < 0.001$ vs. PTX-Veh group, as determined using two-way ANOVA with RM followed by Bonferroni's post hoc multiple comparison test. Veh-Veh, mice received 2 vehicle injections instead of PTX and vinpocetine; PTX-Veh, mice received PTX with a vehicle injection instead of vinpocetine; PTX-Vin, mice received both PTX and vinpocetine.

3.2. Intrathecal application of vinpocetine effectively reduces mechanical hypersensitivity in a CIPN model

Since systemic injection of vinpocetine produced a profound analgesic effect on CIPN, the next experiment was performed to determine whether its analgesic properties could be mediated at the spinal level (Figure 3a).

After the confirmation of full development of CIPN model (Figure 3b; PID3: $p < 0.05$; PID7: $p < 0.001$; for days: $F_{3, 45} = 47.42$, $p < 0.001$; for groups: $F_{2, 15} = 119.8$, $p < 0.001$; for days × groups: $F_{6, 45} = 9.616$, $p < 0.001$, two-way ANOVA with RM followed by Bonferroni's multiple comparison test), vinpocetine was administered i.t. on PID7 and PID14 at a concentration of 143 μM in 10 μl (20 μg/kg), based on the effective i.p. dose of 20 mg/kg and an estimated i.p.-to-i.t. conversion ratio of approximately 100:1, as used in a previous study comparing systemic and spinal administration routes.[49] Baseline von Frey filament test was conducted before vinpocetine administration, and 50% MWTs were measured at 1-, 2-, 4-, and 8 hours post-treatment. On PID7, i.t. administration of vinpocetine significantly increased 50% MWT compared to the PTX-Veh group, showing a time course similar to that observed with systemic injection beginning at 1 and 2 hours post-treatment and persisting up to 4 hours (Figure 3c; 1 h: $p < 0.05$; 2 h and 4 h: $p < 0.001$; for time: $F_{4, 60} = 5.080$, $p < 0.01$; for groups: $F_{2, 15} = 175.6$, $p < 0.001$; for time × groups: $F_{8, 60} = 3.854$, $p < 0.001$, two-way ANOVA with RM followed by Bonferroni's multiple comparison test). By 8 hours, 50% MWT returned to levels comparable to the PTX-Veh group. The results observed on PID14 were consistent with those on PID7, showing that the antinociceptive effect of vinpocetine became evident at 1 hour, peaked at 2 hours, and remained significant until 4 hours before it retreated to baseline (Figure 3d, 1 h: $p < 0.05$, 2 h and 4 h: $p < 0.01$; for time: $F_{4, 60} = 3.569$, $p < 0.05$; for groups: $F_{2, 15} = 142.0$, $p < 0.001$;

for time × groups: $F_{8, 60} = 3.869$, $p < 0.001$, two-way ANOVA with RM followed by Bonferroni's multiple comparison test).

Taken together, these results showed that intrathecal application of vinpocetine effectively alleviates CIPN-induced mechanical hypersensitivity, indicating that the analgesic effect of vinpocetine may, at least in part, be due to action at the spinal cord level.

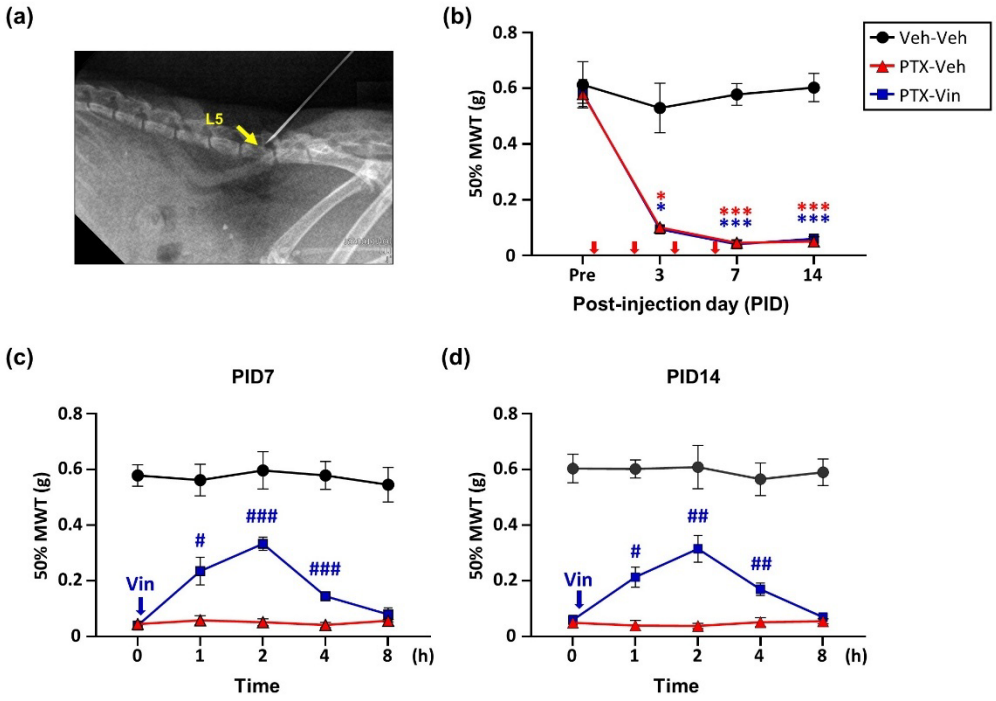

Figure 3. Effects of intrathecal administration of vinpocetine on mechanical hypersensitivity in CIPN model. (a) X-ray confirmation of the intrathecal injection site. Yellow arrow indicates the lumbar 5 (L5) spine. (b) Development of mechanical hypersensitivity following repeated PTX injections. Both PTX-treated groups (PTX-Veh and PTX-Vin) exhibited a significant reduction in 50% MWTs from PID3 to PID14 (n = 6 per group). Red arrows indicate PTX injections. (c) Analgesic effect of intrathecal vinpocetine on PID7. The blue arrow indicates vinpocetine administration. A significant increase in 50% MWTs was observed from 1 to 4 h, peaking at 2 h. (d) Analgesic effect of intrathecal vinpocetine application on PID14. The 50% MWTs in the PTX-Vin group significantly increased from 1 h to 4 h, with the strongest effect at 2 h. Data are presented as mean ± SEM. $^{*}P < 0.05$, $^{***}p < 0.001$ vs. Veh-Veh group, $^{\#}p < 0.05$, $^{\#\#}p < 0.01$, and $^{\#\#\#}p < 0.001$ vs. PTX-Veh group, as determined using two-way ANOVA with RM followed by Bonferroni's post hoc

multiple comparison test. Veh-Veh, mice received 2 vehicle injections instead of PTX and vinpocetine; PTX-Veh, mice received PTX with a vehicle injection instead of vinpocetine; PTX-Vin, mice received both PTX and vinpocetine.

3.3. Repeated vinpocetine treatment alleviates mechanical, thermal, and cold hypersensitivity in a CIPN model

Based on prior experiments, vinpocetine dosages of 5 mg/kg, 10 mg/kg, and 20 mg/kg were chosen for subsequent experiments. To assess whether the analgesic effects of vinpocetine on CIPN can be persisted by daily treatment, vinpocetine was administered daily over a total of 7 days from PID7 to PID13 in the CIPN model. Mechanical, thermal, and cold sensitivity were measured before vinpocetine injection on PID9, PID11, PID13, and PID14 (Figure 4a). Body weights were also measured throughout the experiment to monitor the potential side effects of repeated treatments with PTX and/or vinpocetine.

While no significant changes in body weight were observed among groups (Figure 4b), daily vinpocetine treatment resulted in significantly increased 50% MWTs from PID9 compared to the PTX-Veh group (Figure 4c; 5 mg/kg: $p < 0.05$, 20 mg/kg: $p < 0.001$; two-way ANOVA with RM followed by Bonferroni's multiple comparison test). As shown on PID11 and PID13, the daily vinpocetine treatment maintained its effect in reducing mechanical hypersensitivity in a dose-dependent manner (In the 5 mg/kg PTX-Vin group, PID11: $p < 0.001$, PID13: $p < 0.01$; In the 10 mg/kg PTX-Vin group, PID11: $p < 0.01$, PID13: $p < 0.001$; In the 20 mg/kg PTX-Vin group, PID11: $p < 0.001$, PID13: $p < 0.001$; two-way ANOVA with RM followed by Bonferroni's multiple comparison test). Notably, Data on PID14 showed that the analgesic effect of vinpocetine was sustained over 1 day even after cessation of vinpocetine on PID13 (In the 5 mg/kg PTX-Vin group: $p < 0.01$; In the 10 mg/kg and 20 mg/kg PTX-Vin groups: $p < 0.001$, two-way ANOVA with RM followed by Bonferroni's multiple comparison test).

When PWL was measured to assess thermal hypersensitivity using Hargreaves method, PTX-injected mice displayed significantly shorter PWL than vehicle-treated mice (Veh-Veh group), confirming the development of thermal hypersensitivity (Figure 4d, $p < 0.01$; for days: $F_{6, 270} = 40.75$, $p < 0.001$; for groups: $F_{4, 45} = 55.53$, $p < 0.001$; for days × groups: $F_{24, 270} = 5.464$, two-way ANOVA with RM followed by Bonferroni's multiple comparison test). Thermal hypersensitivity on PID9 was significantly suppressed in a dose-dependent manner in vinpocetine-treated mice compared to that in the PTX-Veh group (In the 5 mg/kg PTX-Vin group, $p < 0.05$; In the 10 and 20 mg/kg PTX-Vin groups, $p < 0.01$, two-way ANOVA with RM followed by Bonferroni's multiple comparison test). The dose-dependent

inhibitory effects of vinpocetine were also shown on PID11 and PID13 (On PID11, $p < 0.001$; On PID13, $p < 0.01$; two-way ANOVA with RM followed by Bonferroni's multiple comparison test). Consistent with those of mechanical sensitivity, the significant inhibition of thermal hypersensitivity also lasted up to PID14, 1 day after discontinuation of vinpocetine (In the 5 and 10 mg/kg PTX-Vin groups, $p < 0.01$; In the 20 mg/kg PTX-Vin group, $p < 0.001$; two-way ANOVA with RM followed by Bonferroni's multiple comparison test).

To further evaluate whether cold hypersensitivity, as well as thermal and mechanical hypersensitivity, was suppressed by vinpocetine, paw withdrawal responses to acetone (in percentage) were measured before PTX injection (Pre) and on PID3 and PID7. PTX-treated groups exhibited significantly increased responses compared to the Veh-treated group, indicating the development of cold hypersensitivity (Figure 4e, PID3 and PID7: $p < 0.001$; for days: $F_{6, 270} = 79.04$, $p < 0.001$; for groups: $F_{4, 45} = 45.96$, $p < 0.001$; for days × groups: $F_{24, 270} = 10.92$; two-way ANOVA with RM followed by Bonferroni's multiple comparison test). Daily vinpocetine treatment showed a marked reduction in responses compared to the PTX-Veh group (PID9: In the 5 mg/kg PTX-Vin group, $p < 0.01$; In the 10 and 20 mg/kg PTX-Vin group, $p < 0.001$; two-way ANOVA with RM followed by Bonferroni's multiple comparison test). The inhibition persisted on PID11 and PID13 across all doses (5, 10, and 20 mg/kg) (In the 5 mg/kg PTX-Vin group, PID11: $p < 0.001$, PID13: $p < 0.01$; In the 10 mg/kg PTX-Vin group, PID11 and PID13: $p < 0.001$; In the 20 mg/kg, PID11: $p < 0.001$, PID13: $p < 0.01$; two-way ANOVA with RM followed by Bonferroni's multiple comparison test). Although a slight increase in responses in vinpocetine-treated mice was observed on PID14, it remained significantly lower in the vinpocetine-treated groups than in the PTX-Veh group ($p < 0.001$, two-way ANOVA with RM followed by Bonferroni's multiple comparison test).

Taken together, the results showed that daily treatment of vinpocetine effectively alleviated mechanical, thermal, and cold hypersensitivity in a dose-dependent manner in the CIPN model.

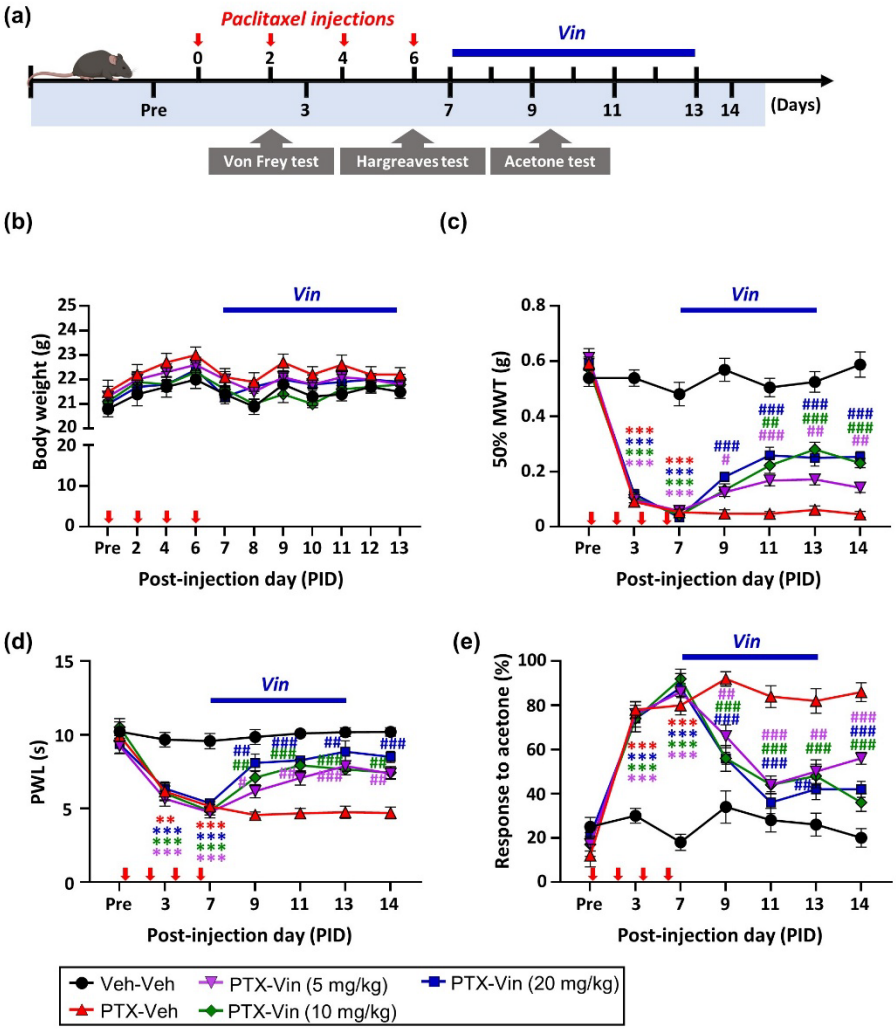

Figure 4. Effects of daily vinpocetine treatment on mechanical, thermal and cold hypersensitivity in the CIPN model. (a) Experimental timeline for vinpocetine treatment and behavioral assessments using von Frey filament, Hargreaves, and acetone methods. (b) Changes in body weight over time. Red arrows indicate PTX injections, while blue bars represent the period of daily vinpocetine application from PID7 to PID13. No significant differences were observed among the groups (n = 10 per group). (c) Analgesic effect of vinpocetine on mechanical hypersensitivity assessed with von Frey filaments. After the pain developed, the 50% MWTs in the PTX-Vin (10

mg/kg) and PTX-Vin (20 mg/kg) groups significantly increased after repeated application of vinpocetine from PID7 to PID13. (d) Analgesic effect of vinpocetine on thermal hypersensitivity assessed using the Hargreaves test. PWL significantly increased in vinpocetine-treated groups (5, 10, and 20 mg/kg) from PID9 to PID14 compared to the PTX-Veh group. (e) Analgesic effect of vinpocetine on cold hypersensitivity assessed by the acetone method. Repeated treatment of vinpocetine at doses of 5, 10, and 20 mg/kg significantly alleviated paw withdrawal responses to acetone. Data are presented as mean ± SEM. $^{**}P < 0.01$, $^{***}p < 0.001$ vs. Veh-Veh group, $^{\#}p < 0.05$, $^{\#\#}p < 0.01$, and $^{\#\#\#}p < 0.001$ vs. PTX-Veh group, as determined using two-way ANOVA with RM followed by Bonferroni's post hoc multiple comparison test. Veh-Veh, mice received 2 vehicle injections instead of PTX and vinpocetine; PTX-Veh, mice received PTX with a vehicle injection instead of vinpocetine; PTX-Vin, mice received both PTX and vinpocetine.

3.4. Vinpocetine alleviated mechanical hypersensitivity in an antimycin A-induced pain model

Antimycin A (A.A) accelerates superoxide production in neurons by inhibiting mitochondrial complex III. It was reported that intrathecal injections of A.A induced pain in mice.[50] Superoxide derived from mitochondria in dorsal horn neurons of the spinal cord is recognized as the primary ROS responsible for the mediation of persistent pain (Figure 5a). To explore the modulation of spinal mitochondrial superoxide in the analgesic effect of vinpocetine, the effect of intrathecal vinpocetine was assessed in an intrathecal A.A-induced pain model.[51,52] 50 μM of A.A was administered i.t.. After 8 hours of A.A administration, the 50% MWT of the A.A-injected group significantly decreased compared to those of the vehicle group (Figure 5b, for time: $F_{1, 15} = 137.6$, $p < 0.001$; for groups: $F_{2, 15} = 32.16$, $p < 0.001$; for time × groups: $F_{2, 15} = 21.37$, $p < 0.001$, two-way ANOVA with RM followed by Bonferroni's multiple comparison test), indicating the successful induction of pain.

When vinpocetine was administered i.t. in A.A-injected mice (Figure 5c), vinpocetine-injected mice (A.A-Vin group) revealed higher 50% MWT 1hour after vinpocetine treatment than the control mice (A.A-Veh group) ($p < 0.05$; for time: $F_{4, 60} = 25.55$, $p < 0.001$; for groups: $F_{2, 15} = 48.92$, $p < 0.001$; for time × groups: $F_{8, 60} = 8.940$, $p < 0.001$, two-way ANOVA with RM followed by Bonferroni's multiple comparison test). Notably, at the 2-h time point, the A.A-Vin group continued to exhibit significantly higher 50% MWTs compared to the A.A-Veh group ($p < 0.05$, two-way ANOVA with RM followed by Bonferroni's multiple comparison test). These results suggest that vinpocetine might alleviate pain by reducing mitochondrial ROS production in the spinal cord.

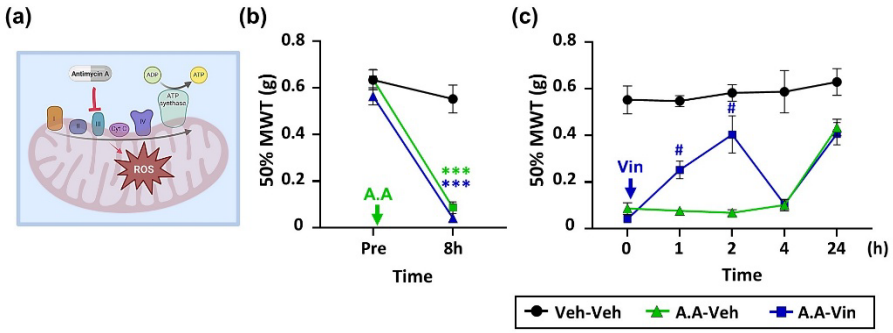

Figure 5. Pain-relieving effect of vinpocetine in an antimycin A-induced pain model. (a) A schematic diagram illustrating the function of antimycin A (A.A) in mitochondria. A.A inhibits mitochondrial complex III and accelerates excessive production of reactive oxygen species (ROS), especially superoxide. (b) A.A- induced pain was fully developed within 8 hours after A.A injection ($p < 0.001$, n = 6 per group). (c) Intrathecal application of vinpocetine alleviated A.A-induced pain, while the A.A-Vin group showed a significant decrease in 50% MWTs at 1 hour ($p < 0.05$), with peak effect at 2 hours ($p < 0.05$). Data are presented as mean ± SEM. $^{***}P < 0.001$ vs. Veh-Veh group, $^{\#}p < 0.05$ vs. A.A-Veh group, as determined using two-way ANOVA with RM followed by Bonferroni's post hoc multiple comparison test. Veh-Veh, mice received 2 vehicle injections instead of A.A and vinpocetine; A.A-Veh, mice received A.A with a vehicle injection instead of vinpocetine; A.A-Vin, mice received both A.A and vinpocetine.

3.5. Intrathecal vinpocetine reduces mechanical hypersensitivity in a KO_2-induced pain model

To further evaluate whether the antinociceptive effect of vinpocetine at the spinal cord level is mediated through scavenging superoxide anions, a superoxide-mediated pain model was built by i.t. injection of the superoxide anion donor potassium superoxide (KO_2),[53] and the effect of vinpocetine was then estimated. The 50% MWTs were assessed using the von Frey filament test at designated time points: baseline (-1 h), immediately before KO_2 administration (0 h), and post-KO_2 injection at 0.5, 1, 1.5, 2, and 4 h (Figure 6a).

An i.t. injection of KO_2 significantly lowered 50% MWTs 0.5 hour after injection compared to the control group, indicating the development of pain (Figure 6b, $p < 0.001$, KO_2-Veh group vs. Veh-Veh group; for time: $F_{6, 90} = 5.985$, $p < 0.001$; for groups: $F_{2, 15} = 5.034$, $p < 0.05$; for time × groups: $F_{12, 90} = 2.914$, $p < 0.01$, two-way ANOVA with RM

followed by Bonferroni's multiple comparison test). However, the pain behaviors were almost completely prevented by an i.t. injection of vinpocetine 1 hour prior to KO_2, showing blockade of KO_2-induced pain by vinpocetine ($p < 0.01$, KO_2-Vin group vs. KO_2-Veh group, two-way ANOVA with RM followed by Bonferroni's multiple comparison test). The antinociceptive effect of vinpocetine lasted up to 1 hour ($p < 0.05$, KO_2-Vin group vs. KO_2-Veh group) and returned to baseline levels over 2 hours. Thus, these results showed that vinpocetine effectively prevented superoxide-mediated pain behaviors by acting at the spinal cord level.

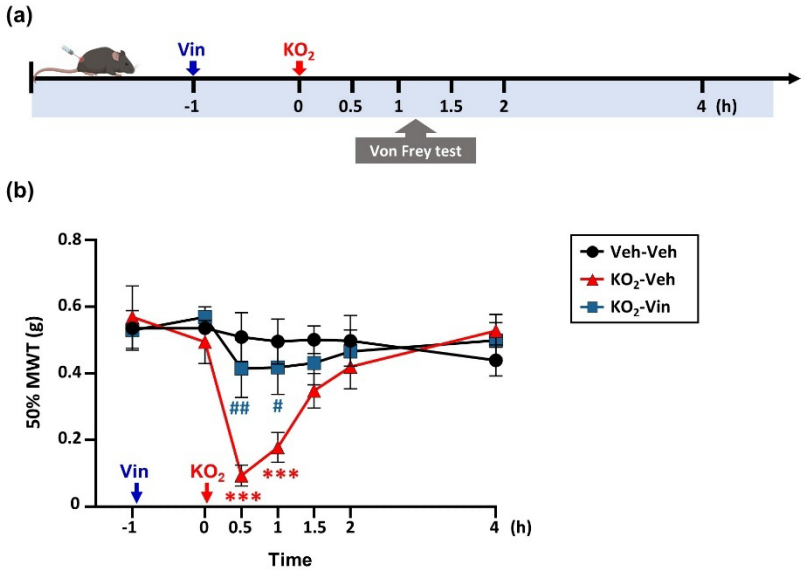

Figure 6. Analgesic effect of vinpocetine in the potassium superoxide (KO_2)-induced pain model. (a) Experimental timeline of drug application and von Frey filament test. (b) Intrathecal injection of vinpocetine alleviated KO_2-induced mechanical hypersensitivity. Pain was observed 0.5 h after KO_2 administration and lasted for approximately 1 hour, with a significant reduction in 50% MWT in the KO_2-Veh group compared to the Veh-Veh group ($p < 0.001$, $n = 6$). Vinpocetine treatment (KO_2-Vin) significantly increased 50% MWT at 0.5 hours ($p < 0.01$, $n = 6$) and 1 hour ($p < 0.05$) after KO_2 injection compared to the KO_2-Veh group. Data are presented as mean ± SEM. $^{***}P < 0.001$ vs. Veh-Veh group, $^{\#}p < 0.05$, $^{\#\#}p < 0.01$ vs. KO_2-Veh group, as determined using two-way ANOVA with RM followed by Bonferroni's post hoc multiple comparison test. Veh-Veh, mice received 2 vehicle injections instead of KO_2 and vinpocetine; KO_2-Veh, mice received KO_2 with a vehicle injection instead of vinpocetine; KO_2-Vin, mice received both KO_2 and vinpocetine.

3.6. Repeated vinpocetine treatment mitigates oxidative stress by decreasing mitochondrial ROS and restoring SOD2 expression

To evaluate whether vinpocetine reduces mitochondrial superoxide production in the spinal dorsal horn neurons of CIPN model, mitochondrial superoxide levels using MitoSOX dye was measured. Additionally, the expression of SOD2, a key enzyme responsible for scavenging superoxide, was analyzed using Western blot. Based on the behavioral results showing that daily treatment with vinpocetine at 20 mg/kg exhibited the most pronounced analgesic effect, another set of mice received daily vinpocetine at 20 mg/kg according to the schedule in Figure 4a, and spinal cords were taken out on PID14 for analysis of mitochondrial superoxide level and SOD2 in the spinal dorsal horn.

When the lamina III-V layers of the spinal cord were examined, oxidized MitoSOX labeling as red fluorescent granules dispersed across the cytoplasmic area was observed (Figure 7a). The density of red granules varied among the experimental groups, prompting quantification of fluorescence intensity (Figure 7b, for groups: $F_{2, 21} = 14.45$, $p < 0.001$, one-way ANOVA followed by Tukey's multiple comparison test). The red fluorescent intensity of labeled cells with MitoSOX in the spinal dorsal horn of PTX-treated mice significantly increased compared to the Veh-Veh group ($p < 0.001$, one-way ANOVA followed by Tukey's multiple comparison test), which was reduced in the mice given daily vinpocetine treatment ($p < 0.05$, one-way ANOVA followed by Tukey's multiple comparison test). In Western blot analysis, the expression level of SOD2 in the spinal cord was lower in the PTX-treated mice than in the Veh-Veh group (Figure 7c, $p < 0.01$; $F_{2, 18} = 12.54$, one-way ANOVA followed by Tukey's multiple comparison test). Notably, the expression of SOD2 in the PTX-Vin group was restored to higher levels than those observed in the PTX-Veh group ($p < 0.01$; one-way ANOVA followed by Tukey's multiple comparison test).

These findings indicate that vinpocetine alleviates pain behaviors by reducing mitochondrial superoxide production and restoring impaired SOD2 in the spinal cord dorsal horn of PTX-treated mice.

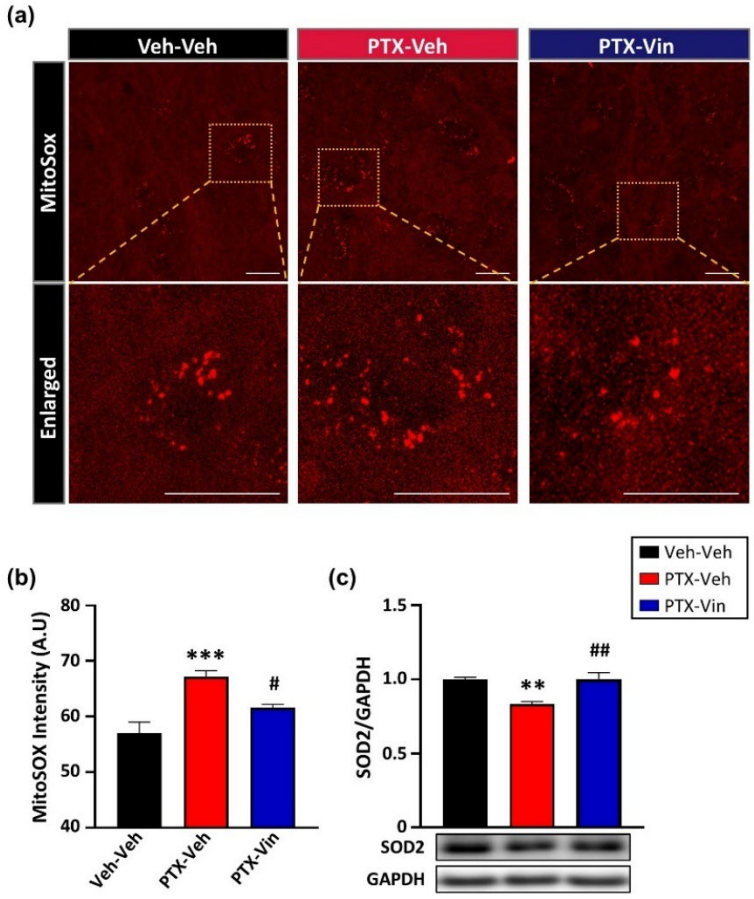

Figure 7. Effect of daily vinpocetine treatment on MitoSOX staining and SOD2 expression in the spinal cord dorsal horn of the CIPN model. (a) Representative fluorescence images of spinal cord sections labeled with MitoSOX to detect mitochondrial ROS levels. Scale bar = 20 μm. (b) Quantification of MitoSOX intensity in the spinal cord among the groups. The PTX-Veh group showed a significant increase compared to the Veh-Veh group ($p < 0.001$, $n = 8$). In contrast, MitoSOX intensity was significantly decreased in the PTX-Vin group compared to that in the PTX-Veh group ($p < 0.05$, $n = 8$). (c) Western blot analysis of SOD2 protein expression in the spinal cord dorsal horn. The SOD2 expression level in the PTX-Veh group was significantly decreased compared to the Veh-Veh group ($p < 0.01$, $n = 7$), but it was significantly increased in the PTX-Vin group compared to the PTX-Veh group ($p < 0.01$, $n = 7$). Data are presented as mean ± SEM. $^{**}P < 0.01$, $^{***}p < 0.001$ vs. Veh-Veh group, $^{\#}p < 0.05$, and $^{\#\#}p < 0.01$ vs. PTX-Veh group, as determined

using one-way ANOVA followed by Tukey's post hoc multiple comparison test. Veh-Veh, mice received 2 vehicle injections instead of PTX and vinpocetine; PTX-Veh, mice received PTX with a vehicle injection instead of vinpocetine; PTX-Vin, mice received both PTX and vinpocetine.

3.7. Daily vinpocetine treatment restores the impaired mitochondrial biogenesis in the spinal cord through the PGC-1α/NRF1/TFAM pathway in the CIPN model

It is known that PGC-1α is an important regulator of mitochondrial biogenesis,[54] and as the downstream signals of PGC-1α, NRF1 and TFAM are involved in mitochondrial DNA replication, transcription, and maintenance.[55] To evaluate the effects of vinpocetine on mitochondrial biogenesis in the spinal cord, the expression of PGC-1α, NRF1, and TFAM was compared in the spinal dorsal horns among the groups. These analyses were conducted on PID14 following repeated vinpocetine treatment (20 mg/kg).

The expression levels of PGC-1α in the PTX-Veh group showed a decrease compared to those in the Veh-Veh group (Figure 8a; $p < 0.05$; For groups, $F_{2, 15} = 5.451$, $p < 0.05$, one-way ANOVA followed by Tukey's multiple comparison test). However, PGC-1α levels were significantly upregulated in the PTX-Vin group compared to the PTX-Veh group ($p < 0.05$; For groups, $F_{2, 15} = 4.023$, $p < 0.05$, one-way ANOVA followed by Tukey's multiple comparison test). This suggests that vinpocetine may counteract the inhibitory effects of PTX on PGC-1α expression. Meanwhile, the expression of NRF1, a downstream factor of PGC-1α, was decreased in the PTX-Veh group compared to that in the Veh-Veh group (Figure 8b; $p < 0.01$; For groups, $F_{2, 18} = 6.645$, $p < 0.01$, one-way ANOVA followed by Tukey's multiple comparison test). However, NRF1 levels were significantly upregulated in the PTX-Vin group relative to the PTX-Veh group ($p < 0.05$, one-way ANOVA followed by Tukey's multiple comparison test). As NRF1 directly regulates mitochondrial DNA transcription and replication through TFAM, the expression levels of TFAM were further examined (Figure 8c). TFAM levels in the PTX-Veh group were reduced compared to those in the Veh-Veh group, indicating that PTX treatment suppresses TFAM expression ($p < 0.001$; For groups, $F_{2, 15} = 16.66$, $p < 0.001$, one-way ANOVA followed by Tukey's multiple comparison test). However, consistent with NRF1, TFAM levels were significantly upregulated in the PTX-Vin group compared to the PTX-Veh group ($p < 0.01$, one-way ANOVA followed by Tukey's multiple comparison test). These results showed that repeated vinpocetine treatment promotes mitochondrial biogenesis in the spinal cord dorsal horn by restoring the impaired PGC-1α and downstream targets NRF1 and TFAM in the CIPN model and thus attenuates pain behaviors.

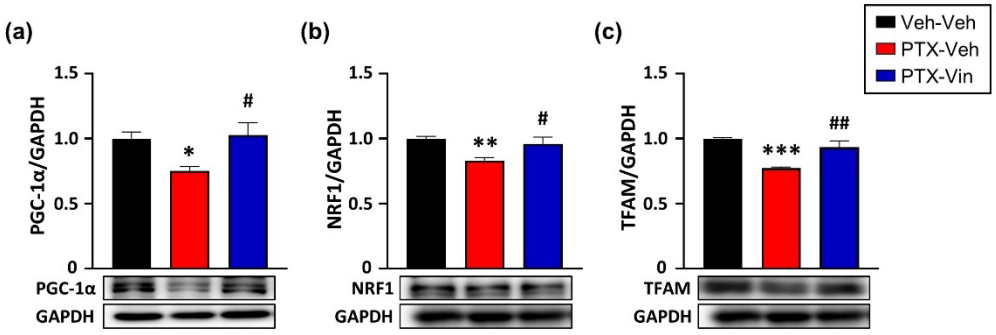

Figure 8. Effect of daily vinpocetine treatment on expression of mitochondrial biogenesis-related factors in the spinal cord of the CIPN model. (a) The expression level of PGC-1α was significantly decreased compared to that in the Veh-Veh group ($p < 0.05$, $n = 8$ per group). However, the expression level of PGC-1α was significantly higher in the PTX-Vin group compared to the PTX-Veh group ($p < 0.05$). (b) NRF1, a downstream factor of PGC-1α, was downregulated in the PTX-Veh group compared to the Veh-Veh group ($p < 0.01$, $n = 7$ per group). However, it was significantly upregulated in the PTX-Vin group compared to that in the PTX-Veh group ($p < 0.05$). (c) The expression level of TFAM, a downstream factor of NRF1, was lower in the PTX-Veh group than in the Veh-Veh group ($p < 0.001$, $n = 6$ per group). Notably, TFAM levels were significantly higher in the PTX-Vin group compared to the PTX-Veh group ($p < 0.01$). Data are presented as mean ± SEM. $^{**}P < 0.01$, $^{***}p < 0.001$ vs. Veh-Veh group, $^{\#}p < 0.05$, and $^{\#\#}p < 0.01$ vs. PTX-Veh group, as determined using one-way ANOVA followed by Tukey's post hoc multiple comparison test.

3.8. Determination of the threshold for CIPN-induced hyperexcitability in the spinal cord dorsal horn by optical imaging

To investigate the impact of CIPN on neuronal excitability, voltage-sensitive dye imaging (VSDI) was performed on spinal cord slices on PID14 in the CIPN model-a time point when the model had stabilized, ensuring reproducible and reliable measurements of neuronal hyperexcitability. Given the limited references on performing VSDI in the spinal cord, minimal electrical stimulation intensity was required to distinguish neuronal responses between CIPN and normal mice. After 1-hour incubation with VSD, the dye was washed out with aCSF. An electrode was positioned to target the dorsal horn of the spinal cord, specifically around lamina II, and was inserted approximately 80 μm deep.

Stimulation intensities started at 0.1 mA and increased incrementally by 0.1 mA. A 10-minute recovery interval was implemented between trials, with continuous flow of aCSF. After the recovery period, recordings were performed for the next set of parameters.

Green fluorescence in the optical images in Figure 9a showed the activated area of the dorsal horn following incremental stimulation intensities.

While 0.1-0.2 mA stimulation intensities revealed no significant differences in stimulation-induced activated areas between Veh and PTX groups, the stimulation intensities more than 0.3 mA showed significantly enhanced neuronal responses in the PTX-treated group compared to the Veh group (Figure 9b, $p < 0.01$, unpaired t-test), indicating a threshold causing neuronal hyperexcitability in the spinal dorsal horn of CIPN mice. When stimulation-induced peak amplitudes were analyzed, stimulation intensities over 0.3 mA tended to increase peak amplitudes compared to the Veh group (Figure 9c, $p < 0.05$, unpaired t-test). As intensities over 0.3 mA showed significant differences in both the activated areas and peak amplitudes between CIPN and vehicle mice, a threshold of 0.3 mA was used for the following experiments.

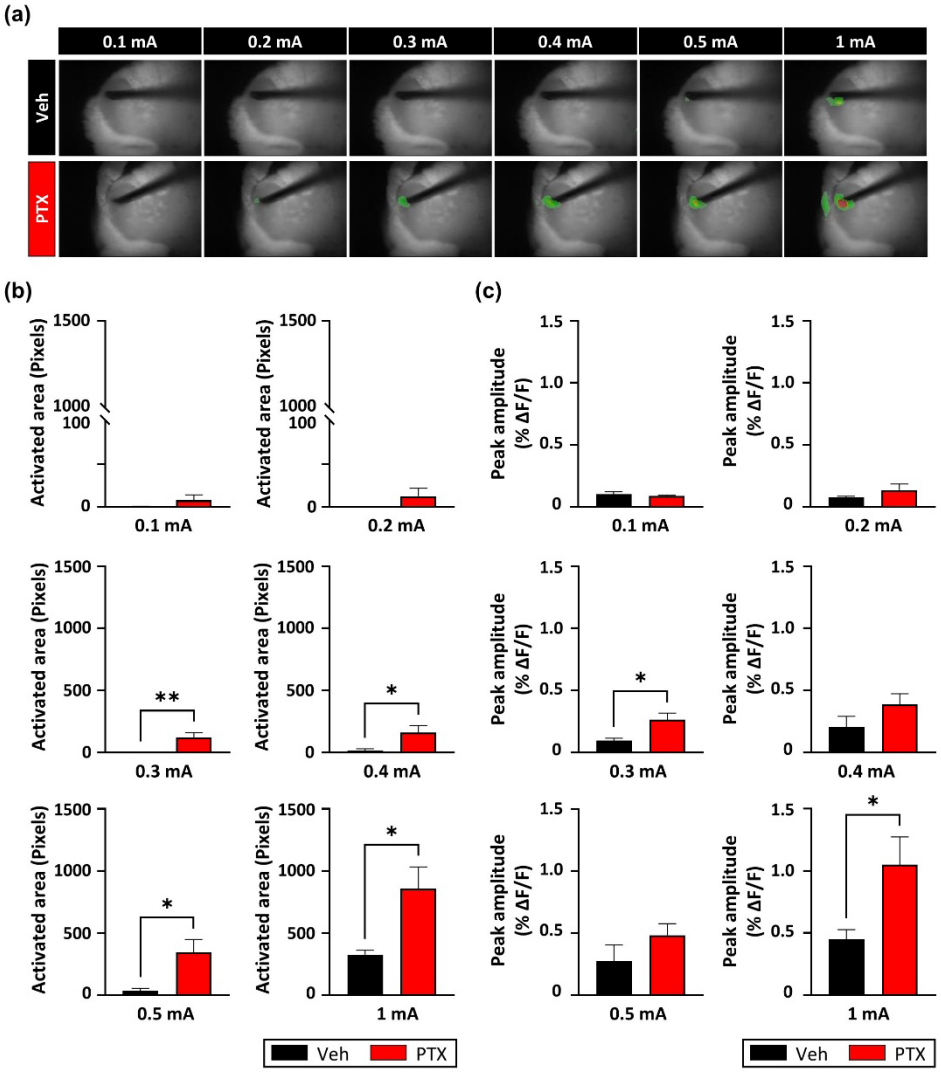

Figure 9. Comparison of peak amplitudes and activated areas by electrical stimulation of the spinal cord dorsal horns between the vehicle and paclitaxel-treated groups in VSDI. (a) Representative images showing higher neuronal activation (green) following incremental stimulation intensities in the spinal dorsal horn of the Veh and PTX groups. (b) Comparison of stimulation-induced activation areas in the spinal dorsal horns between the Veh and PTX groups. The PTX group showed significantly larger activated area over an intensity of 0.3 mA than Veh

group ($p < 0.01$ in 0.3 mA, n = 6, $p < 0.05$ in 0.4 mA, n = 6; $p < 0.05$ in 0.5 mA, n = 6; $p < 0.05$ in 1 mA, n = 6). (c) Comparison of stimulation-induced peak amplitudes between Veh and PTX groups. The PTX group exhibited a significantly higher peak amplitude compared to the Veh group at the stimulation intensity of 0.3 mA ($p < 0.05$, n = 6) and 1 mA ($p < 0.05$, n = 6). Data are presented as mean ± SEM. $^{*}P < 0.05$, $^{**}p < 0.01$ vs. Veh group, as determined using an unpaired t-test.

3.9. Vinpocetine treatment reduces stimulation-induced neuronal activity in the spinal cord dorsal horn of the CIPN model

As the prior experiment determined a stimulation of threshold of 0.3 mA for detecting neuronal hyperexcitability, the next experiments used the stimulation intensities of 0 mA, 0.3 mA, 0.6 mA and 1.2 mA for electrical stimulation of spinal dorsal horns and evaluated the effect of vinpocetine on stimulation-induced neuronal activity in the CIPN model. VSDI following each intensity stimulation was taken before (Pre), immediately after incubation (Treat), and after washing out (Post) vinpocetine or vehicle (DMSO). Vinpocetine or DMSO was applied in the chamber for 15 minutes to allow full interaction with the spinal cord slice (Figure 10a).

The peak amplitude at each stimulation intensity was compared across groups (Pre, Treat, and Post phases). At 0, 0.3, and 0.6 mA stimulation intensities, there were no significant differences between the DMSO- and Vin-treated groups in all phases. In the treatment phase of 0, 0.3, and 0.6 mA stimulations, the Vin-treated group showed a slight decrease in peak amplitude, but no significant differences were observed when compared to the DMSO group (Figure 10b). However, at 1.2 mA stimulation, the Vin-treated group showed a significant decrease in peak amplitude compared to the DMSO group during the treatment phase ($p < 0.01$; For phases: $F_{2, 32} = 6.536$, $p < 0.01$; for groups: $F_{1, 16} = 0.7808$, $p > 0.05$; for phases × groups: $F_{2, 32} = 6.697$, $p < 0.01$, two-way ANOVA with RM followed by Bonferroni's multiple comparison test), while no differences were observed in the Pre and Post phases.

To further evaluate neuronal activity over time, Area Under the Curve (AUC) analysis was conducted separately for each stimulation intensity and each phase in both the DMSO and Vin groups. The treatment phase was highlighted with shaded color to distinguish it from the Pre and Post phases at each stimulation intensity (Figure 10c). At 0 mA stimulation, almost no signals were detected (Figure 10c, DMSO_0 mA and Vin_0 mA; Figure 10d, 0 mA). At 0.3 mA stimulation, the DMSO group showed minimal changes in AUC across all three phases (Figure 10b, DMSO_0.3 mA). In contrast, in the Vin-treated group, the AUC in the line graph showed a reduction in the shaded area during the treatment phase compared to the Pre and Post phases (Figure 10c, Vin_0.3 mA). However, when comparing

the AUC between the DMSO and Vin groups, there were no significant differences (Figure 10d, 0.3 mA). At 0.6 mA stimulation, the results were similar to those at 0.3 mA, with no significant differences in AUC between the DMSO and Vin-treated groups (Figure 10c, DMSO_0.6 mA, Vin_0.6 mA; Figure 10d, 0.6 mA). However, at 1.2 mA stimulation, while the DMSO group showed no significant differences between phases, the Vin-treated group exhibited a dramatic decrease in the AUC during the treatment phase compared to the Pre-phase. In the Post-phase, the AUC slightly increased but remained lower than that in the Pre-phase. When comparing AUC between the DMSO and Vin-treated groups, a significant reduction was observed in the Vin-treated group (Figure 10d, 1.2 mA; $p < 0.05$, For phases: $F_{2, 32} = 4.775$, $p < 0.05$; for groups: $F_{1, 16} = 1.125$, $p > 0.05$; for phases × groups: $F_{2, 32} = 5.765$, $p < 0.01$, two-way ANOVA with RM followed by Bonferroni's multiple comparison test). Taken together, these results indicate that vinpocetine treatment reduces neuronal activity in a stimulation-dependent manner, with significant effects observed at higher stimulation intensities (1.2 mA).

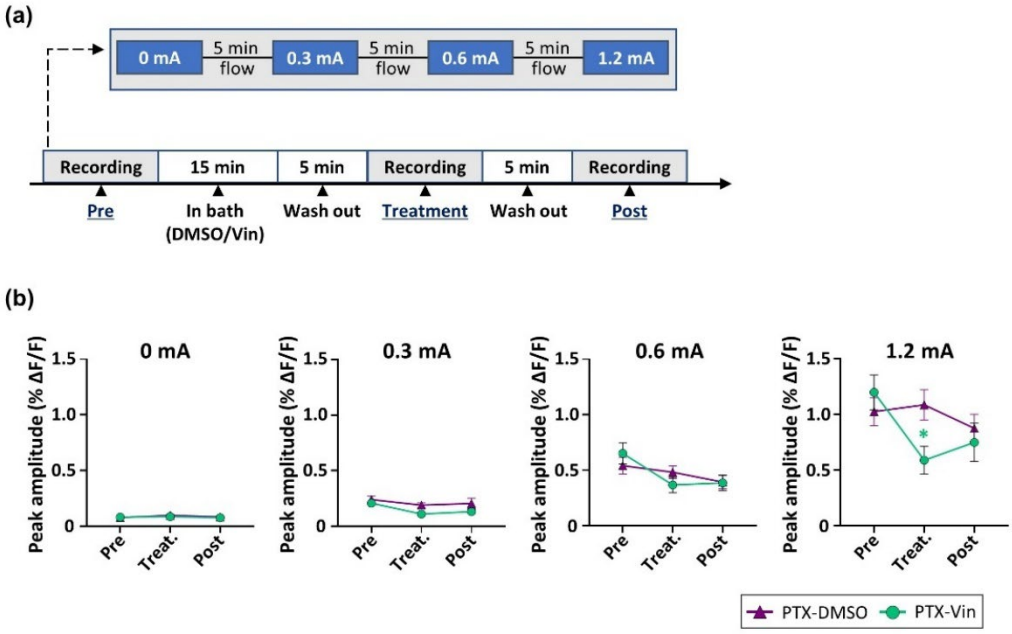

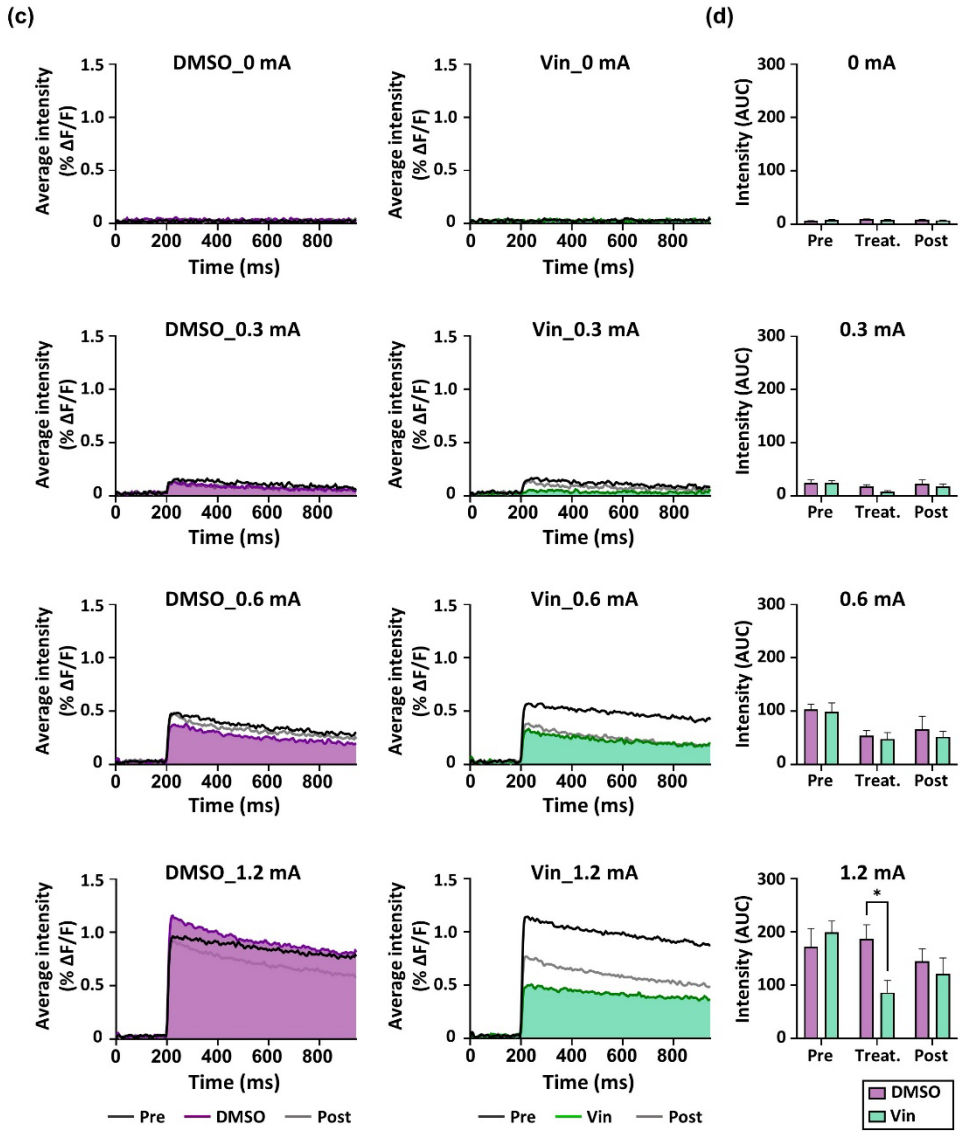

Figure 10. Effects of vinpocetine on the neuronal excitability induced by various stimulation intensities in the spinal dorsal horns of CIPN model. (a) Schematic view of the experimental procedure used in VSDI. The recording process consisted of three phases: the pre-treatment phase (before DMSO or vinpocetine administration), the treatment phase (DMSO or vinpocetine

treatment), and the post-treatment phase. Each recording follows a sequential stimulation protocol of 0, 0.3, 0.6, and 1.2 mA, with a 5-minute flow period between each stimulation. (b) Comparison of peak amplitude across pre-treatment, treatment, and post-treatment phases in the DMSO- and vinpocetine (Vin) groups. At a stimulation intensity of 1.2 mA, the Vin group showed a significant decrease in peak amplitude compared to the DMSO group ($p < 0.05$, $n = 9$). (c) Changes in average intensity over time. The average intensity refers to the amplitude corresponding to each time point. Data are shown separately for each group, with pre-treatment, treatment, and post-treatment phase changes presented together. In particular, the treatment phases in the DMSO and Vin groups were highlighted with color. The area under the curve (AUC) from 200 ms to 943.5 ms is displayed for each electrical stimulation intensity. (d) Comparison of stimulation-evoked AUC between the DMSO and Vin groups in the pre-treatment, treatment, and post-treatment phases. At a stimulation intensity of 1.2 mA, the AUC in the vinpocetine-treated group was significantly smaller than that in the DMSO group ($p < 0.05$, $n = 9$). Data are presented as mean ± SEM. $^{*}P < 0.05$ vs. DMSO group, as determined using two-way ANOVA followed by Bonferroni's post hoc multiple comparison test.

3.10. Vinpocetine maintains neuronal activity inhibition for over 2 hours in spinal cord slices

Since the optical imaging data indicated that the decreased neuronal activity did not recover quickly, a 2-hour phase (2 h-phase) was added following vinpocetine application in the bath (Figure 11a). This adjustment was based on behavioral test results, which demonstrated that the antinociceptive effect significantly declined 2 hours after reaching its peak on PID 14 (Figure 2d).

The changes in neuronal activity across different phases and stimulation intensities are shown in Figure 11b. During the treatment phase, under 0.6 mA and 1.2 mA electrical stimulation, the Vin group exhibited reduced neuronal activity compared to the DMSO group.

To determine the statistical differences among each phase, data were analyzed by assessing the peak amplitude changes across the experimental phases for each group, with the results categorized based on the stimulation intensity. Additionally, comparisons between groups were analyzed (Figure 11c). At 0 mA, no significant phase-dependent changes were observed in either group. At 0.3 mA, the DMSO group exhibited no noticeable changes, whereas the Vin group showed a significant reduction in peak amplitude during the treatment phase (Treat-phase, $p < 0.01$; for phases, $F_{3, 24} = 4.142$, $p < 0.05$; for groups: $F_{1, 8} = 1.210$, $p > 0.05$; for phases × groups: $F_{3, 24} = 5.973$, $p < 0.01$, two-way ANOVA with RM followed by Bonferroni's multiple comparison test), followed by a recovery trend in the Post-phase and 2 h-phase, with no significant difference from the Pre-

phase. The difference between the Vin and DMSO groups was significant in the Treat-phase, with the Vin group showing a significantly higher peak amplitude than the DMSO group ($p < 0.01$, two-way ANOVA with RM followed by Bonferroni's multiple comparison test). At 0.6 mA, the peak amplitude significantly decreased in the Treat-phase ($p < 0.001$; for phases, $F_{3, 24} = 11.25$, $p < 0.001$; for groups: $F_{1, 8} = 1.363$, $p > 0.05$; for phases × groups: $F_{3, 24} = 1.388$, $p > 0.05$, two-way ANOVA with RM followed by Bonferroni's multiple comparison test) and showed a recovery trend in the Post-phase ($p < 0.01$) and 2 h-phase ($p < 0.01$) in the Vin group. However, the values in the Post- and 2h-phases remained significantly lower than those in the Pre-phase, indicating a prolonged effect of vinpocetine. In contrast, the DMSO group showed a slight but statistically insignificant decline across the phases. There was no significant difference between the Vin and DMSO groups. At 1.2 mA, a similar trend in the Vin group was observed with peak amplitude. In the Treat-phase, the peak amplitude was significantly lower than that in the Pre-phase ($p < 0.01$; for phases, $F_{3, 24} = 4.866$, $p < 0.01$; for groups: $F_{1, 8} = 8.927$, $p < 0.05$; for phases × groups: $F_{3, 24} = 3.890$, $p > 0.05$, two-way ANOVA with RM followed by Bonferroni's multiple comparison test). The amplitude increased during the Post- and 2 h-phase compared with the Treat-phase. However, the Post- and 2 h-phase still showed a significant difference from the Pre-phase (In Post-phase, $p < 0.01$; In 2 h phase, $p < 0.05$, two-way ANOVA with RM followed by Bonferroni's multiple comparison test). In contrast, the DMSO group showed no significant changes over time. When comparing the Vin group with the DMSO group, a significant difference was observed in both the Treat-phase ($p < 0.01$) and the Post-phase ($p < 0.05$).

These findings indicate that vinpocetine sustains its effect on reducing neuronal activity for more than 2 hours in spinal cord slices of the CIPN model, with a significant effect observed under 0.6 mA stimulation. While a similar trend was noted at 1.2 mA stimulation, it did not reach statistical significance, suggesting that the effect of vinpocetine may be stimulation-intensity dependent.

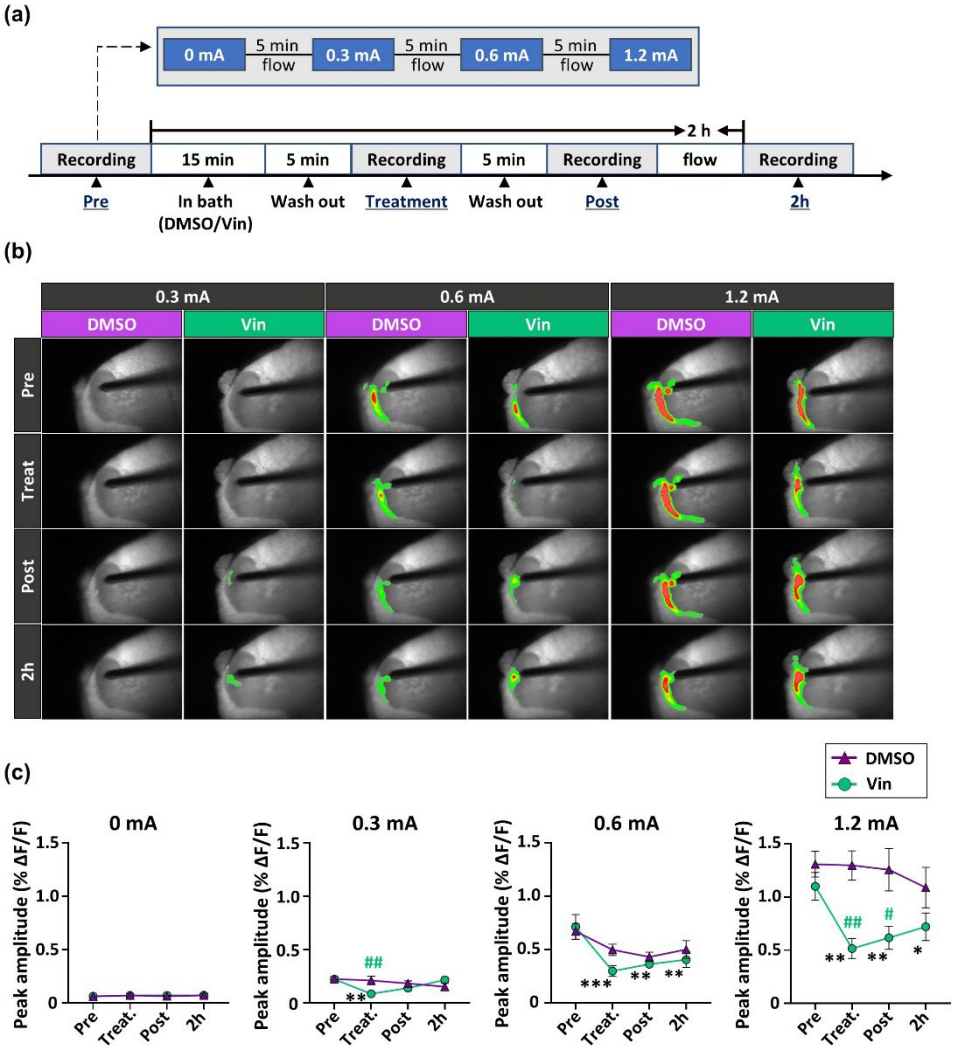

Figure 11. Time-dependent changes in peak amplitudes in the spinal cord dorsal horn of the CIPN model following vinpocetine treatment in the bath. (a) Schematic overview of the experimental procedure used in VSDI. The recording process consisted of four phases: the pre-treatment phase (before DMSO or vinpocetine administration), the treatment phase (DMSO or vinpocetine administration), the post-treatment phase, and the 2h-after treatment phase. Each recording follows a sequential stimulation protocol of 0 mA, 0.3 mA, 0.6 mA, and 1.2 mA, with a 5-minute flow period between each stimulation. Additionally, a continuous flow is maintained

before the 2h-after treatment phase. (b) Representative optical images of the spinal cord in the CIPN model, comparing DMSO- and vinpocetine-treated groups at different stimulation intensities and phases. (c) Comparison of peak amplitude change over time at different electrical stimulation intensities in the DMSO and vinpocetine (Vin) groups. During the treatment phase, vinpocetine significantly reduced peak amplitudes compared to the Pre-phase at 0.3 mA ($p < 0.01$, $n = 5$), 0.6 mA ($p < 0.01$, $n = 5$), and 1.2 mA ($p < 0.05$, $n = 5$). At the 2h phase, the Vin group showed no significant difference from the Pre-phase at 0.3 mA and 1.2 mA. However, a significant reduction persisted at 0.6 mA ($p < 0.05$, $n = 5$). Data are presented as mean ± SEM. $^{*}P < 0.05$, $^{**}p < 0.01$ vs. Pre-phase, $^{\#}p < 0.05$, and $^{\#\#}p < 0.01$ vs. DMSO group, as determined using two-way ANOVA followed by Bonferroni's post hoc multiple comparison test.

3.11. Repeated vinpocetine treatment inhibits AMPA and NR2B expressions in the spinal cord of the CIPN model

To investigate the effect of vinpocetine treatment on the expressions of AMPA, NR2A, and NR2B, which are known to be involved in CIPN-induced maladaptive spinal plasticity, Western blot was performed on PID14 following repeated vinpocetine treatment. Western blot results revealed significant upregulation of AMPA receptor expression in the PTX-Veh group compared to the Veh-Veh group (Figure 12a, $p < 0.01$; for groups, $F_{2, 15} = 8.770$, $p < 0.01$, one-way ANOVA followed by Tukey's multiple comparison test), suggesting enhanced excitatory synaptic transmission in CIPN. However, vinpocetine treatment significantly reduced AMPA receptor expression in the PTX-Vin group ($p < 0.05$, one-way ANOVA followed by Tukey's multiple comparison test), indicating that it may suppress CIPN-induced excitatory synaptic potentiation and restore synaptic homeostasis. In contrast to AMPA receptor changes, NR2A receptor expression remained unchanged between the PTX-Veh and PTX-Vin groups (Figure 12b), suggesting that CIPN-induced synaptic plasticity is not primarily mediated through NR2A-containing NMDA receptors. Similar to AMPA receptor expression, the expression level of NR2B receptors was significantly increased in the PTX-Veh group (Figure 12c, $p < 0.01$; For groups, $F_{2, 15} = 8.603$, $p < 0.01$, one-way ANOVA followed by Tukey's multiple comparison test), suggesting that CIPN enhances NR2B-mediated NMDA receptor signaling, which may contribute to spinal synaptic plasticity and pain sensitization. Notably, vinpocetine treatment significantly reduced NR2B expression in the PTX-Vin group compared to that in the PTX-Veh group ($p < 0.01$, one-way ANOVA followed by Tukey's multiple comparison test), indicating that its analgesic effects may involve the suppression of NR2B-dependent synaptic plasticity and excitatory neurotransmission.

Taken together, these results suggest that CIPN-induced maladaptive spinal plasticity is

characterized by increased AMPA and NR2B receptor expression, which enhances excitatory synaptic transmission and promotes NMDA receptor-dependent pain sensitization. Importantly, vinpocetine treatment effectively attenuated these changes, indicating its potential role in restoring synaptic balance and mitigating CIPN-associated chronic pain by modulating AMPA and NR2B receptor expression.

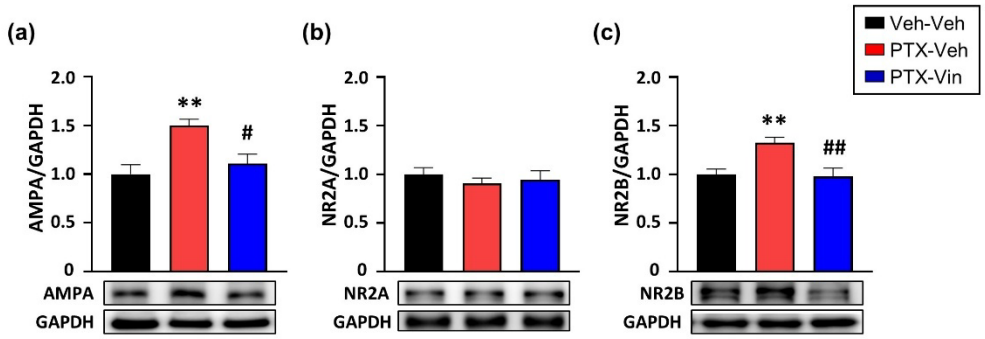

Figure 12. Expression levels of AMPA, NR2A, and NR2B in the spinal cord of the CIPN model following repeated vinpocetine treatment. (a) AMPA expression was significantly higher in the PTX-Veh group compared to the Veh-Veh group ($p < 0.01$, $n = 6$), but significantly reduced in the PTX-Vin group ($p < 0.05$, $n = 6$). (b) No significant differences were observed in NR2A expression among the groups ($p > 0.05$, $n = 6$). (c) The expression level of NR2B was markedly elevated in the PTX-Veh group ($p < 0.01$, $n = 6$), while it was significantly decreased following vinpocetine treatment ($p < 0.05$, $n = 6$). Data are presented as mean ± SEM. $^{**}P < 0.01$ vs. Veh-Veh group, $^{\#}p < 0.05$, and $^{\#\#}p < 0.01$ vs. PTX-Veh group, as determined by using one-way ANOVA followed by Tukey's post hoc multiple comparison test.

3.12. AMPA receptor expression in the spinal cord dorsal horn is modulated by vinpocetine treatment

To further confirm the inhibitory effect of vinpocetine on AMPA receptor expression in the CIPN model, immunohistochemistry staining for AMPA receptors in the spinal dorsal horn neurons of the CIPN model was performed. The distribution of AMPA receptors appeared denser in the superficial dorsal horn (Figure 13a), particularly within 150 μm from the dorsal root entry zone, which was selected for quantitative analysis. Mean fluorescence intensity analysis revealed an increase in AMPA receptor expression in the PTX-Veh group compared to the Veh-Veh group (Figure 13b, $p < 0.001$; For groups, $F_{2, 105} = 42.82$, $p < 0.001$, one-way ANOVA followed by Tukey's multiple comparison test). In

contrast, the PTX-Vin group displayed a decrease in AMPA receptor expression compared to the PTX-Veh group ($p < 0.001$, one-way ANOVA followed by Tukey's multiple comparison test).

To further explore whether AMPA receptor expression is specifically altered in spinal cord neurons, colocalization analysis with NeuN, a neuronal marker, was performed. The results showed that in the PTX-Veh group, the colocalization area of AMPA with NeuN-positive neurons was significantly increased compared to that in the Veh-Veh group (Figure 13c, $p < 0.001$; For groups, $F_{2, 105} = 36.72$, $p < 0.001$, one-way ANOVA followed by Tukey's multiple comparison test). However, in the PTX-Vin group, the colocalization area showed a decrease compared to that in the PTX-Veh group ($p < 0.05$, one-way ANOVA followed by Tukey's multiple comparison test).

These findings suggest that PTX treatment enhances AMPA receptor expression in spinal cord neurons, particularly in NeuN-positive neurons, while vinpocetine treatment may partially attenuate this effect.

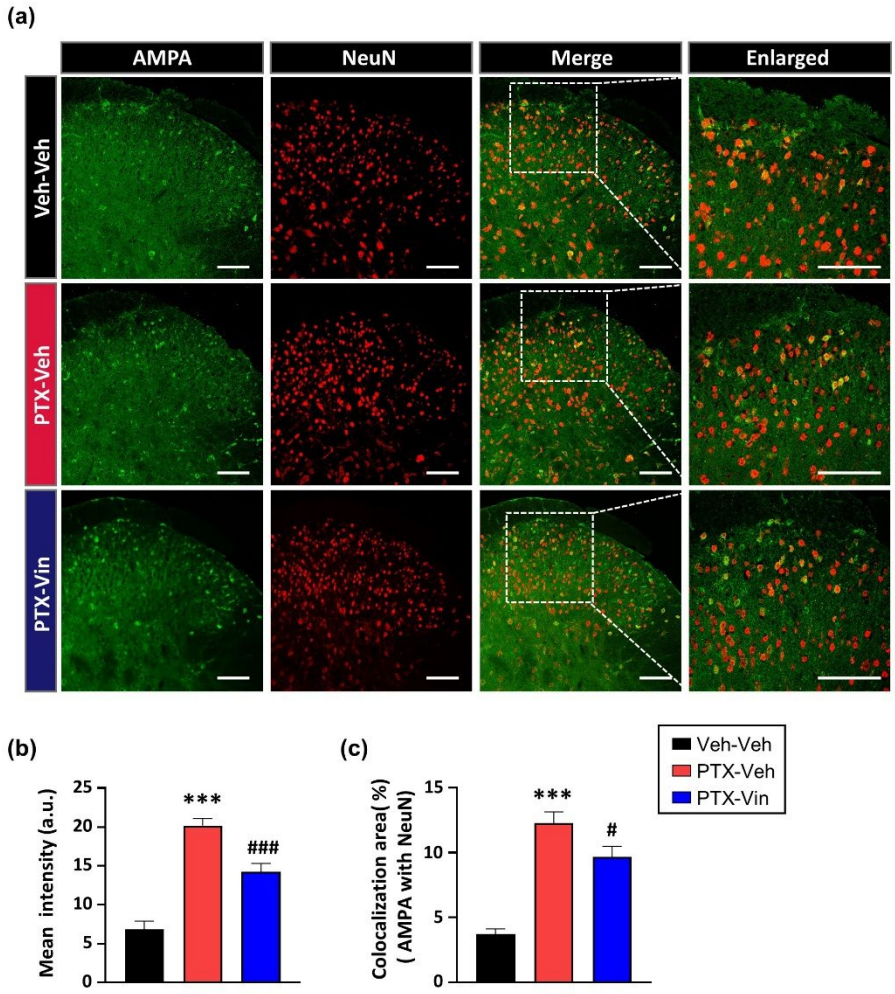

Figure 13. Inhibition by vinpocetine treatment of enhanced expression of AMPA in the spinal dorsal horn neurons of CIPN model. (a) Representative confocal microscopy images of AMPA receptor (green) and NeuN (red) expression in the spinal cord dorsal horn from different groups. Merged images (yellow) indicate the colocalization of AMPA with NeuN. The enlarged images correspond to the areas outlined by the white squares in the merged images. (b) Quantification of the mean fluorescence intensity of AMPA in the dorsal horn (n = 6 per group). The mean intensity of AMPA in the PTX-Veh group showed significant increase compared to the Veh-Veh group ($p < 0.001$), while the PTX-Vin group showed a significant decrease compared to the PTX-Veh group ($p < 0.001$). (c) Quantification of the colocalization area of AMPA with NeuN in each group. The PTX-

Veh group showed a significant increase in colocalized areas compared to the Veh-Veh group ($p < 0.001$). The PTX-Vin group exhibited a decrease relative to the PTX-Veh group ($p < 0.05$). Scale bar = 100 μm. Data are presented as mean ± SEM. $^{***}P < 0.001$ vs. Veh-Veh group, $^{\#}p < 0.05$, $^{\#\#\#}p < 0.001$ vs. PTX-Veh group, as determined by using one-way ANOVA followed by Tukey's post hoc multiple comparison test.

3.13. Vinpocetine regulates PKC-α expression in the spinal cord of the CIPN model

Given that enhanced expression of AMPA receptors was attenuated by vinpocetine treatment, intracellular protein kinases, including PKC-α, CaMKII-α, and PKA, were further examined. PKC-α and CaMKII-α are known to enhance AMPA receptor function through phosphorylation,[56] whereas PKA modulates AMPA receptor trafficking and synaptic plasticity.[57] To assess these molecular changes, Western blot was conducted on PID14 following repeated vinpocetine treatment.

Western blot analysis revealed that PKC-α expression was significantly increased in the CIPN spinal cord compared to that in the Veh-Veh group (Figure 14a, $p < 0.01$; For groups, $F_{2, 15} = 9.150$, $p < 0.01$, one-way ANOVA followed by Tukey's multiple comparison test). However, vinpocetine treatment led to a marked reduction in PKC-α levels compared to the CIPN group ($p < 0.01$, one-way ANOVA followed by Tukey's multiple comparison test). This suggests that vinpocetine may exert its effects through an AMPA-PKC-α-dependent mechanism in the spinal cord. The expression of CaMKII-α showed no significant differences between the PTX-Veh group and Veh-Veh group (Figure 14b). Vinpocetine treatment did not significantly alter CaMKII-α expression, indicating that its levels remained stable across conditions, suggesting that CaMKII-α is not significantly affected in this model. Similarly, PKA expression showed no significant differences among the three groups (Figure 14c). This indicated that vinpocetine did not have a notable effect on PKA expression in this model.

These findings suggest that vinpocetine primarily modulates AMPA receptor expression in the CIPN spinal cord through the AMPA-PKC-α pathway, while its influence on CaMKII-α and PKA signaling appears to be limited or requires further investigation.

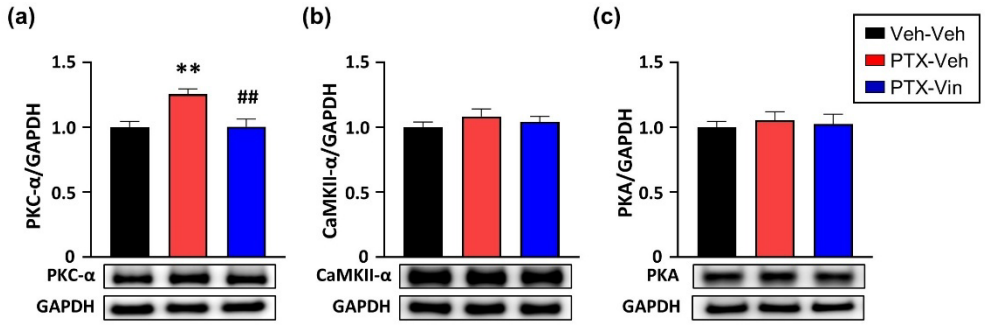

Figure 14. Expression of PKC-α, CaMKII-α, and PKA in the spinal cord of the CIPN model following repeated vinpocetine treatment. (a) PKC-α expression was significantly increased in the PTX-Veh group compared to that in the Veh-Veh group ($p < 0.01$, $n = 6$), but significantly reduced in the PTX-Vin group ($p < 0.05$, $n = 6$). (b) CaMKII-α expression showed no differences among the groups ($p > 0.05$, $n = 8$) (c) PKA expression showed no significant differences among groups ($p > 0.05$, $n = 8$). Data are presented as mean ± SEM. $^{**}P < 0.01$ vs. Veh-Veh group, $^{\#\#}p < 0.01$ vs. PTX-Veh group, as determined by using one-way ANOVA followed by Tukey's post hoc multiple comparison test.

3.14. Vinpocetine modulates PKC-α spatial distribution in the spinal cord dorsal horn of CIPN mice

Previous studies using Western blot analysis demonstrated an increase in PKC-α expression in CIPN conditions, which was attenuated by vinpocetine treatment. To further examine the spatial distribution of PKC-α expression, immunohistochemistry staining was performed in the spinal cord dorsal horn. The results revealed a distinctive expression pattern, with intense green fluorescence signals of PKC-α observed primarily in the superficial dorsal horn (Figure 15a).

To quantify these changes, the mean fluorescence intensity of PKC-α was analyzed and compared among the experimental groups. The results showed that the fluorescence intensity was significantly higher in the PTX-Veh group compared to the Veh-Veh group (Figure 15b, $p < 0.001$; for groups, $F_{2, 123} = 18.69$, $p < 0.001$, one-way ANOVA followed by Tukey's multiple comparison test). Similarly, the PTX-Vin group exhibited a significant reduction in fluorescence intensity compared to the PTX-Veh group. ($p < 0.01$, one-way ANOVA followed by Tukey's multiple comparison test).

To further investigate whether changes in PKC-α expression occurred specifically in neurons, colocalization analysis with NeuN was performed (Figure 16a). The results demonstrated that in the PTX-Veh group, the colocalization area of PKC-α with NeuN-positive neurons was significantly increased compared to that in the Veh-Veh group (Figure 16b, $p < 0.05$; for groups, $F_{2, 58} = 4.684$, $p < 0.05$, one-way ANOVA followed by Tukey's multiple comparison test). Notably, the PTX-Vin group exhibited a significant decrease in the colocalization area compared to the PTX-Veh group ($p < 0.05$, one-way ANOVA followed by Tukey's multiple comparison test).

These findings suggest that PKC-α expression is upregulated in CIPN, particularly in spinal cord neurons, and vinpocetine treatment effectively reduces this upregulation.

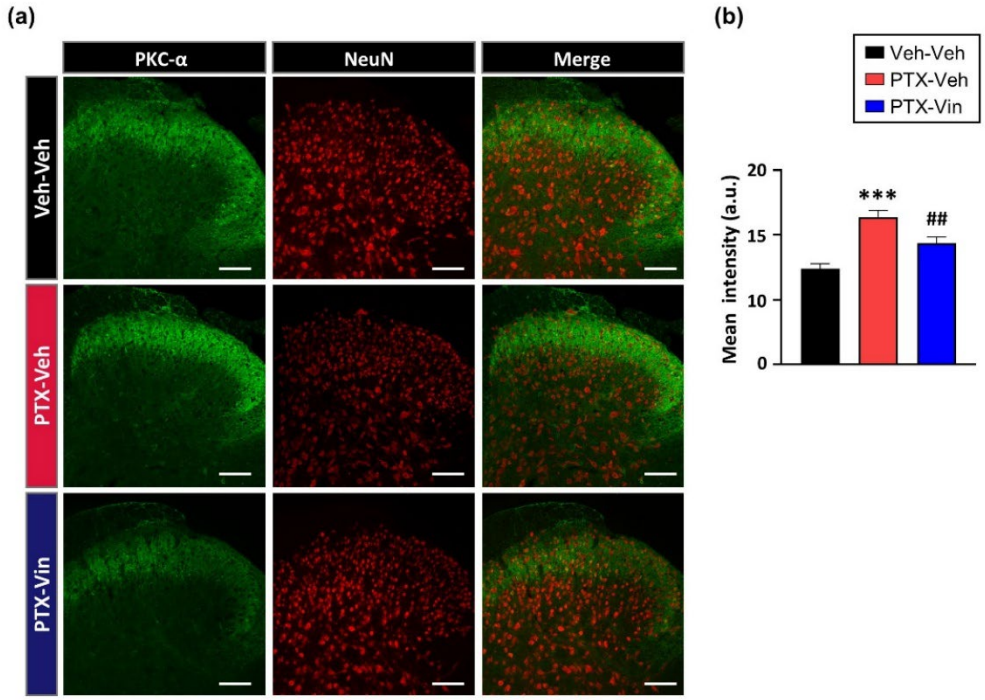

Figure 15. PKC-α expression in the spinal cord dorsal horn following repeated vinpocetine treatment. (a) Representative confocal microscopy images of PKC-α (green) and NeuN (red) expression in the spinal dorsal horn across the experimental groups. Colocalization of merged images indicates colocalization between PKC-α and NeuN. (b) Quantification of the mean fluorescence intensity of PKC-α in the superficial dorsal horn (n = 6 per group). The PTX-Veh group exhibited an increase in PKC-α expression compared to that in the Veh-Veh group ($p < 0.001$). The mean intensity of PKC-α expression in the PTX-Vin group was higher than that in the PTX-Veh group ($p < 0.01$). Scale bar = 100 μm. Data are presented as mean ± SEM. $^{***}P < 0.001$ vs. Veh-Veh group, $^{\#\#}p < 0.01$ vs. PTX-Veh group, as determined by using one-way ANOVA followed by Tukey's post hoc multiple comparison test.

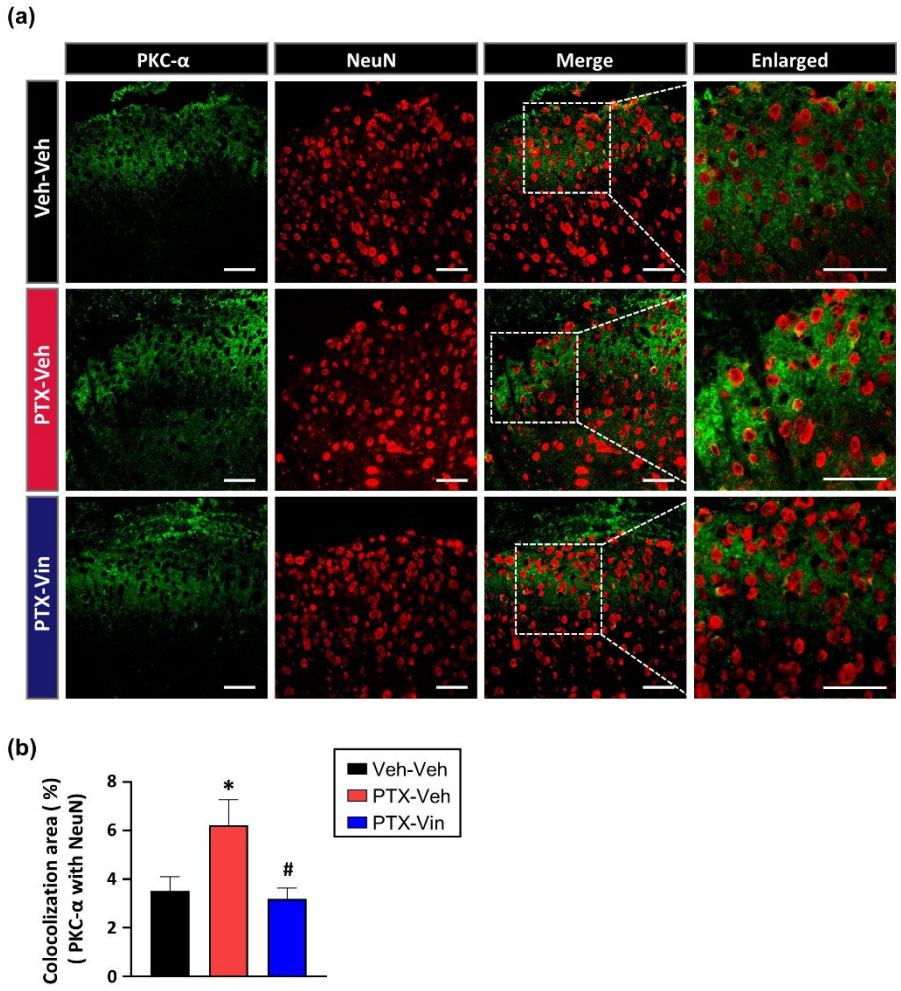

Figure 16. Colocalization of PKC-α expression with NeuN-positive neurons in the spinal cord dorsal horn following repeated administration of vinpocetine. (a) Representative confocal microscopy images of PKC-α (green) and NeuN (red) expression in the spinal dorsal horn across the experimental groups. Merged images (yellow) indicate the colocalization of PKC-α with NeuN. The enlarged images correspond to the areas outlined by the white squares in the merged images. (b) Quantification of the colocalization area of PKC-α with NeuN in each group (n = 6 in per group). The PTX-Veh group showed a significant increase compared to the Veh-Veh group ($p < 0.05$). The PTX-Vin group exhibited significant downregulation compared to the PTX-Veh group ($p < 0.05$).

Scale bar = 50 μm. Data are presented as mean ± SEM. $^{*}P < 0.05$ vs. Veh-Veh group, $^{\#}p < 0.05$ vs. PTX-Veh group, as determined by using one-way ANOVA followed by Tukey's post hoc multiple comparison test.

4. Discussion

CIPN is a major dose-limiting side effect and a form of neuropathic pain associated with potentially curative cancer chemotherapy,[58] characterized by sensory abnormalities such as tingling, burning pain, and numbness, which can progress to chronic pain and motor dysfunction.[59] These symptoms involve multiple pathophysiological mechanisms, including oxidative stress, mitochondrial dysfunction, and neuroinflammation, which lead to central sensitization, dysregulated pain signaling, and ultimately, neuronal hyperexcitability.[60] Despite its high prevalence and significant impact on quality of life in patients and on treatment outcomes, effective therapeutic options remain limited. In this study, the pain-relieving mechanisms of vinpocetine in CIPN were investigated, focusing on its effects on oxidative stress through regulating mitochondrial biogenesis, as well as its role in modulating central sensitization in the spinal cord. The present results demonstrated that vinpocetine effectively alleviates mechanical hypersensitivity in a CIPN model, with the most pronounced effect at 20 mg/kg. Intrathecal administration of vinpocetine further confirmed its efficacy in modulating spinal cord pain processing. Vinpocetine reduced mitochondrial ROS levels, restored SOD2 expression, and promoted mitochondrial biogenesis through the PGC-1α/NRF1/TFAM pathway in CIPN. Furthermore, vinpocetine treatment suppressed neuronal hyperactivity and the enhanced expressions of AMPA and NR2B receptors, and PKC-α in spinal dorsal horn neurons induced by paclitaxel therapy. Collectively, these findings suggest that vinpocetine produces profound analgesic effects on pain behaviors in the CIPN model by reducing oxidative stress, enhancing mitochondrial function, and suppressing central sensitization in the spinal cord dorsal horn. Notably, this study is the first to demonstrate its role in promoting mitochondrial biogenesis via the PGC-1α/NRF1/TFAM pathway in a CIPN model, providing novel insights into mitochondrial function and pain modulation.

4.1. Analgesic effects of vinpocetine in a CIPN model

The analgesic effects of vinpocetine were evaluated in a paclitaxel-induced CIPN model, a widely used preclinical model that closely mimics the neuropathic pain observed in chemotherapy patients.[61] Paclitaxel disrupts microtubule dynamics, leading to axonal degeneration, mitochondrial dysfunction, and oxidative stress accumulation.[62] Given that oxidative stress and mitochondrial dysfunction are central contributors to CIPN pathophysiology,[63] this model provides a relevant platform to assess the therapeutic potential of vinpocetine. In this model, behavioral assessments were conducted, focusing

on its impact on mechanical hypersensitivity, thermal hypersensitivity, and cold hypersensitivity.

To determine the optimal dosing regimen, vinpocetine at varying concentrations was administered intraperitoneally as a single administration on PID7 and PID14, followed by assessment of mechanical hypersensitivity was assessed at these time points. Previous studies have shown that CIPN progresses through distinct phases, with PID7 representing an early stage, and PID14 reflecting a more established neuropathic condition. These phases exhibit different pain sensitivities, which could influence treatment efficacy.[64] By selecting these two time points, the aim was to capture the temporal evolution of CIPN symptoms and evaluate whether the efficacy of vinpocetine differs between early and late phases of the condition. Behavioral tests revealed that vinpocetine significantly alleviated mechanical hypersensitivity at both time points in a dose-dependent manner, with 20 mg/kg producing the most significant effect. This suggests that vinpocetine exerts acute analgesic effects in CIPN, although its duration of action was limited to less than four hours, indicating the need for repeated administration to sustain its efficacy. Thus, repeated administration of vinpocetine from PID7 to PID13 was performed to investigate its potential for sustained pain relief. The effects were assessed across multiple pain modalities, including mechanical, thermal, and cold hypersensitivity. Repeated administration was performed to evaluate cumulative analgesic effects, as sustained drug exposure is often required to maintain therapeutic efficacy in neuropathic conditions.[65] These assessments were conducted to provide a comprehensive evaluation of the impact of vinpocetine on different sensory modalities, as CIPN is known to involve complex alterations in pain processing.[66] The repeated administration of vinpocetine led to a significant and prolonged reduction in pain behaviors, suggesting that continuous treatment may be necessary to achieve optimal therapeutic effects in CIPN.

Based on the dose-response findings from systemic administration, the most effective concentration was selected for intrathecal injection testing. Intrathecal administration was employed to determine whether the analgesic effects of vinpocetine could be directly mediated at the spinal cord level, further elucidating its potential mechanisms of action. Intrathecal administration of vinpocetine at a selected dose produced robust pain relief, reinforcing the notion that vinpocetine modulates central pain processing in CIPN. Collectively, these findings demonstrate that vinpocetine provides both immediate and prolonged pain relief in CIPN, with its effectiveness being modulated by dose, treatment duration, and the route of administration.

4.2. Vinpocetine exhibits analgesic effects in oxidative stress-induced pain models

Oxidative stress plays a crucial role in the pathogenesis of neuropathic pain, including CIPN, by inducing mitochondrial dysfunction, increasing ROS production, and triggering neuroinflammation.[21,67] A.A and KO_2 have been widely used to model oxidative stress-induced neuropathic pain due to their ability to impair mitochondrial electron transport and increase oxidative damage.[50,68] These models provide a useful platform for evaluating the therapeutic potential of antioxidants such as vinpocetine.

In this study, intrathecal administration of vinpocetine significantly reduced mechanical hypersensitivity in both A.A- and KO_2-induced pain models. This suggests that vinpocetine exerts its analgesic effects by counteracting oxidative stress and mitigating mitochondrial dysfunction. Given the known pharmacological properties of vinpocetine, its neuroprotective and antioxidant effects may underlie its ability to alleviate oxidative stress-associated neuropathic pain. Previous studies have demonstrated that vinpocetine acts as a phosphodiesterase-1 (PDE1) inhibitor and modulates calcium homeostasis, which may contribute to its protective effects against oxidative stress-induced neuronal damage.[69] Notably, inhibition of PDE1 has been implicated in enhancing mitochondrial function and reducing oxidative burden in neuronal cells, suggesting an additional mechanism by which vinpocetine may exert its analgesic effects.[70] Furthermore, oxidative stress induces direct neuronal injury and disrupts cellular homeostasis, leading to increased pain sensitivity.[71,72] The attenuation of pain behavior in these oxidative stress-induced models suggests that vinpocetine may exert its effects primarily through the regulation of oxidative stress and mitochondrial function. Collectively, these studies highlight the importance of targeting oxidative stress in neuropathic pain management and suggest that vinpocetine could serve as a potential therapeutic candidate for oxidative stress-related pain conditions.

These findings align with previous reports demonstrating that targeting oxidative stress pathways can effectively mitigate neuropathic pain.[73-75] By significantly reducing pain hypersensitivity in oxidative stress-induced pain models, vinpocetine has emerged as a promising candidate for addressing oxidative damage-related neuropathic conditions beyond CIPN.

4.3. Vinpocetine modulates mitochondrial oxidative stress and enhances mitochondrial biogenesis in CIPN

Given the well-established role of mitochondrial dysfunction in CIPN, the potential

mechanism of vinpocetine in restoring mitochondrial homeostasis may involve reducing oxidative stress and enhancing mitochondrial biogenesis. Mitochondrial dysfunction in CIPN has been linked to increased ROS production and impaired antioxidant defense mechanisms, leading to neuronal damage and heightened pain sensitivity.[76] MitoSOX staining revealed a significant reduction in mitochondrial ROS levels in the spinal cord following repeated vinpocetine treatment, confirming its role in reducing oxidative stress-associated neuropathy. This reduction in oxidative stress is critical, as excessive ROS generation is associated with mitochondrial dysfunction, activation of pro-apoptotic pathways, and sustained pain signaling.[38] By decreasing ROS levels, vinpocetine may help maintain mitochondrial integrity. This suggests that vinpocetine mitigates oxidative stress at the mitochondrial level, potentially preventing neuronal damage and pain hypersensitivity.

To further investigate the pain modulation mechanism in the spinal cord of CIPN mice, key regulators of mitochondrial biogenesis and antioxidant defense were analyzed. The expression level of SOD2, a key mitochondrial antioxidant enzyme that neutralizes mitochondrial ROS,[77] was found to be increased following vinpocetine treatment. The observed increase in SOD2 levels could be attributed to either a reduction in oxidative stress, leading to decreased consumption, or direct modulation of SOD2 expression. Previous studies suggest that mitochondrial oxidative damage can regulate SOD2 activity through post-translational modifications, such as nitration or phosphorylation, which affects its stability and function.[78-80] Additionally, deceased oxidative stress itself can lead to reduced demand for SOD2 expression, as cells may no longer require heightened antioxidant defense under conditions of lower ROS production.[81] Further investigation is required to determine whether vinpocetine influences SOD2 expression directly or through indirect mechanisms by reducing oxidative burden.

In the present study, Western blot analysis demonstrated increased expression of PGC-1α, NRF1, and TFAM following repeated vinpocetine administration, indicating that vinpocetine not only reduces oxidative stress but also enhances mitochondrial biogenesis. PGC-1α is a key regulator of mitochondrial biogenesis, coordinating the transcription of genes essential for mitochondrial replication and function.[82] The upregulation of PGC-1α following vinpocetine treatment indicates enhanced mitochondrial recovery, which may improve cellular resistance to oxidative damage and support sustained neuronal function.[83] Findings from the aforementioned studies suggest that vinpocetine exerts dual effects by both reducing oxidative stress and promoting mitochondrial biogenesis. The increased expression of PGC-1α implies improved mitochondrial biogenesis and function, which may underlie the prolonged analgesic effects of vinpocetine in CIPN. This finding reinforces the role of PGC-1α as a critical regulator of mitochondrial recovery, further

supporting its involvement in vinpocetine-mediated neuroprotection. Collectively, these findings provide evidence that vinpocetine simultaneously mitigates oxidative stress and enhances mitochondrial biogenesis, thereby contributing to its therapeutic effects in CIPN. These results suggest that the prolonged analgesic effects of vinpocetine may be attributed to its capacity to enhance mitochondrial resilience, optimize cellular energy production, and alleviate pain hypersensitivity over time.

4.4. Vinpocetine regulates spinal cord excitability in CIPN

To investigate the effects of vinpocetine on spinal cord excitability, VSDI was performed on L4 spinal cord slices obtained from CIPN models on PID14, following a single application of vinpocetine in the bath solution. VSDI provides a real-time assessment of neuronal activity, making it a valuable technique for evaluating changes in spinal cord excitability associated with pain modulation.[84] 0.3 mA was identified as the optimal stimulation threshold for VSDI in the spinal cord of CIPN mice, a critical parameter for standardizing electrophysiological assessments in neuropathic pain research. This threshold determination provides a valuable reference for future research utilizing the VSDI in CIPN models, ensuring consistency in assessing spinal cord excitability changes due to chemotherapy-induced neurotoxicity, neuronal damage, and functional impairment.

After establishing this threshold, the effects of vinpocetine were examined at 0.3, 0.6, 1.2 mA electrical stimulation intensities and found that vinpocetine significantly reduced spinal cord neuronal activity in a stimulation-dependent manner. The most pronounced suppression was observed at 1.2 mA, indicating that vinpocetine effectively counteracts CIPN-associated hyperexcitability. These findings reinforce the role of vinpocetine in modulating central sensitization and pain processing, likely by attenuating excessive neuronal firing and reducing spinal cord hyperexcitability.

4.5. Vinpocetine modulates excitatory synaptic transmission and intracellular signaling in CIPN

To further elucidate the impact of vinpocetine on central sensitization, this study examined key excitatory synaptic receptors and intracellular signaling pathways relevant to pain, with a particular focus on those regulating glutamatergic neurotransmission and synaptic plasticity. Accumulated data indicate that spinal AMPA receptors are essential in the processes of both acute and chronic pain.[85,86] Additionally, the ability of vinpocetine to block NaV1.8 sodium channel activity has been implicated in reducing neuronal

excitability and pain perception.[87] In the present study, Western blot analysis revealed significant downregulation of AMPA and NR2B receptor expression following repeated vinpocetine treatment, whereas NR2A levels remained unchanged. These results suggest that vinpocetine may attenuate long-term potentiation (LTP)-like mechanisms,[88] thereby reducing the persistence of chronic pain. Since AMPA and NR2B receptors are key regulators of synaptic plasticity and LTP, their downregulation suggests that vinpocetine may interfere with excitatory transmission to mitigate pain hypersensitivity, further supporting its role in reducing excitatory synaptic transmission and central sensitization.

Furthermore, IHC analysis demonstrated reduced colocalization of AMPA receptors with NeuN-positive neurons, indicating that vinpocetine not only downregulated AMPA receptor expression but also affected their neuronal localization. This suggests a potential mechanism by which vinpocetine modifies the synaptic architecture to dampen excessive excitatory transmission, further reinforcing its role in alleviating CIPN-associated pain hypersensitivity. Previous studies have indicated that targeting oxidative stress pathways can mitigate neuropathic pain,[89,90] suggesting that the antioxidative effects of vinpocetine may contribute to the downregulation of these excitatory synaptic components.

Additionally, in the present study, PKC-α expression was significantly reduced, whereas CaMKII-α levels showed no significant changes. This selective reduction in PKC-α suggests targeted interference with protein kinase signaling pathways associated with synaptic plasticity and pain hypersensitivity. Given that vinpocetine inhibits NF-κB-dependent inflammatory responses and directly targets inhibitor of NF-κB (IκB) kinase,[91] it is plausible that its effects on PKC-α may contribute to dampening central sensitization. Since PKC-α is involved in AMPA receptor trafficking and phosphorylation,[92] its downregulation may further contribute to reduced synaptic excitability, reinforcing the impact of vinpocetine on excitatory transmission. This indicates that vinpocetine selectively interferes with PKC-α-mediated signaling pathways known to enhance synaptic plasticity and pain hypersensitivity,[93] suggesting a role for vinpocetine in modulating protein kinase-dependent pain mechanisms.

Moreover, IHC analysis demonstrated reduced colocalization of PKC-α with NeuN-positive neurons, supporting the notion that vinpocetine alters the spatial distribution of PKC-α in neuronal circuits. This further suggests that vinpocetine not only downregulates PKC-α expression but also modifies its intracellular localization, potentially disrupting PKC-α-dependent synaptic mechanisms associated with pain hypersensitivity. These results suggest that vinpocetine not only downregulates protein expression but also modifies synaptic architecture, which may further contribute to its antinociceptive effects in CIPN.

4.6. Study limitations and future perspectives

While this study provides novel insights into the role of vinpocetine in modulating oxidative stress, mitochondrial function, and central sensitization in CIPN, several limitations should be acknowledged. The assessment of oxidative stress is primarily focused on mitochondrial superoxide levels, whereas oxidative stress is a multifaceted process involving various ROS, such as hydrogen peroxide (H_2O_2), hydroxyl radicals (•OH), and peroxynitrite ($ONOO^-$). A more comprehensive evaluation incorporating additional oxidative stress markers would further clarify the antioxidative mechanisms of vinpocetine.

Additionally, while vinpocetine has been shown to enhance mitochondrial biogenesis through the PGC-1α/NRF1/TFAM pathway, further validation through genetic knockdown or overexpression studies is required to establish a causal relationship. Moreover, the current study primarily examined mitochondrial ROS without considering the interactions between the mitochondrial and cytosolic ROS pathways, which could play an essential role in neuroinflammation and pain signaling. Future studies should explore a broader redox balance to provide a more integrated understanding of the effects of vinpocetine on the regulation of oxidative stress.

From a translational perspective, although vinpocetine exhibited significant analgesic effects in the CIPN mouse model, further preclinical investigations are required to evaluate its long-term safety, appropriate dosing regimen, and possible interactions with chemotherapeutic drugs. Further investigations using patient-derived neuronal models or clinical trials are crucial to determine its therapeutic applicability in CIPN and other neuropathic pain conditions.

5. Conclusion

The findings of the present study support the potential use of vinpocetine in the treatment of CIPN. Vinpocetine mitigates CIPN by targeting oxidative stress, enhancing mitochondrial biogenesis, and modulating spinal cord excitability. Notably. This study is the first to demonstrate the role of vinpocetine in promoting mitochondrial biogenesis via the PGC-1α/NRF1/TFAM pathway in a CIPN model, thus offering novel insights into the mitochondrial function in pain modulation. Given the limited therapeutic options available for CIPN, this study highlights the potential of vinpocetine as a novel therapeutic strategy for CIPN and provides a foundation for future translational research aimed at improving neuropathic pain management in chemotherapy patients.

References

1. Bae EH, Greenwald MK, Schwartz AG. Chemotherapy-induced peripheral neuropathy: Mechanisms and therapeutic avenues. Neurotherapeutics 2021;18:2384-96.
2. Addington J, Freimer M. Chemotherapy-induced peripheral neuropathy: an update on the current understanding. F1000Res 2016;5.
3. Seretny M, Currie GL, Sena ES, Ramnarine S, Grant R, MacLeod MR, et al. Incidence, prevalence, and predictors of chemotherapy-induced peripheral neuropathy: A systematic review and meta-analysis. Pain 2014;155:2461-70.
4. Ibrahim EY, Ehrlich BE. Prevention of chemotherapy-induced peripheral neuropathy: A review of recent findings. Crit Rev Oncol Hematol. 2020;145:102831.
5. Flatters SJL, Dougherty PM, Colvin LA. Clinical and preclinical perspectives on chemotherapy-induced peripheral neuropathy (CIPN): A narrative review. Br J Anaesth. 2017;119:737-49.
6. Shah A, Hoffman EM, Mauermann ML, Loprinzi CL, Windebank AJ, Klein CJ, et al. Incidence and disease burden of chemotherapy-induced peripheral neuropathy in a population-based cohort. J Neurol Neurosurg Psychiatry 2018;89:636-41.
7. Pike CT, Birnbaum HG, Muehlenbein CE, Pohl GM, Natale RB. Healthcare costs and workloss burden of patients with chemotherapy-associated peripheral neuropathy in breast, ovarian, head and neck, and nonsmall cell lung cancer. Chemother Res Pract. 2012;2012:913848.
8. Desforges AD, Hebert CM, Spence AL, Reid B, Dhaibar HA, Cruz-Topete D, et al. Treatment and diagnosis of chemotherapy-induced peripheral neuropathy: An update. Biomed Pharmacother. 2022;147:112671.
9. Mezzanotte JN, Grimm M, Shinde NV, Nolan T, Worthen-Chaudhari L, Williams NO, et al. Updates in the treatment of chemotherapy-induced peripheral neuropathy. Curr Treat Options Oncol 2022;23:29-42.
10. Argyriou AA, Bruna J, Park SB, Cavaletti G. Emerging pharmacological strategies for the management of chemotherapy-induced peripheral neurotoxicity (CIPN), based on novel CIPN mechanisms. Expert Rev Neurother 2020;20:1005-16.
11. Starobova H, Vetter I. Pathophysiology of chemotherapy-induced peripheral neuropathy. Front Mol Neurosci 2017;10:174.
12. Balayssac D, Cayre A, Authier N, Bourdu S, Penault-Llorca F, Gillet JP, et al. Patterns of P-glycoprotein activity in the nervous system during vincristine-induced neuropathy in rats. J Peripher Nerv Syst 2005;10:301-10.
13. Gu J, Hu M, Gu Z, Yu J, Ji Y, Li L, et al. Bibliometric analysis reveals a 20-year research trend for chemotherapy-induced peripheral neuropathy. Front Neurol 2021;12:793663.
14. Canta A, Pozzi E, Carozzi VA. Mitochondrial dysfunction in chemotherapy-induced peripheral neuropathy (CIPN). Toxics 2015;3:198-223.
15. Guo C, Sun L, Chen X, Zhang D. Oxidative stress, mitochondrial damage and

neurodegenerative diseases. Neural Regen Res 2013;8:2003-14.
16. Tirichen H, Yaigoub H, Xu W, Wu C, Li R, Li Y. Mitochondrial reactive oxygen species and their contribution in chronic kidney disease progression through oxidative stress. Front Physiol 2021;12:627837.
17. Trecarichi A, Flatters SJL. Mitochondrial dysfunction in the pathogenesis of chemotherapy-induced peripheral neuropathy. Int Rev Neurobiol 2019;145:83-126.
18. Waseem M, Kaushik P, Tabassum H, Parvez S. Role of mitochondrial mechanism in chemotherapy-induced peripheral neuropathy. Curr Drug Metab 2018;19:47-54.
19. Fidanboylu M, Griffiths LA, Flatters SJ. Global inhibition of reactive oxygen species (ROS) inhibits paclitaxel-induced painful peripheral neuropathy. PLoS One 2011;6:e25212.
20. Park SE, Neupane C, Noh C, Sharma R, Shin HJ, Pham TL, et al. Antiallodynic effects of KDS2010, a novel MAO-B inhibitor, via ROS-GABA inhibitory transmission in a paclitaxel-induced tactile hypersensitivity model. Mol Brain 2022;15:41.
21. Agnes JP, Santos VWD, das Neves RN, Gonçalves RM, Delgobo M, Girardi CS, et al. Antioxidants improve oxaliplatin-induced peripheral neuropathy in tumor-bearing mice model: Role of spinal cord oxidative stress and inflammation. J Pain 2021;22:996-1013.
22. Singh J, Thapliyal S, Kumar A, Paul P, Kumar N, Bisht M, et al. Dimethyl fumarate ameliorates paclitaxel-induced neuropathic pain in rats. Cureus 2022;14:e28818.
23. Ilari S, Lauro F, Giancotti LA, Malafoglia V, Dagostino C, Gliozzi M, et al. The protective effect of bergamot polyphenolic fraction (BPF) on chemotherapy-induced neuropathic pain. Pharmaceuticals (Basel) 2021;14.
24. Duggett NA, Griffiths LA, Flatters SJL. Paclitaxel-induced painful neuropathy is associated with changes in mitochondrial bioenergetics, glycolysis, and an energy deficit in dorsal root ganglia neurons. Pain 2017;158:1499-508.
25. Chen SD, Yang DI, Lin TK, Shaw FZ, Liou CW, Chuang YC. Roles of oxidative stress, apoptosis, PGC-1alpha and mitochondrial biogenesis in cerebral ischemia. Int J Mol Sci 2011;12:7199-215.
26. Li PA, Hou X, Hao S. Mitochondrial biogenesis in neurodegeneration. J Neurosci Res 2017;95:2025-9.
27. Fontecha-Barriuso M, Martin-Sanchez D, Martinez-Moreno JM, Monsalve M, Ramos AM, Sanchez-Nino MD, et al. The role of PGC-1alpha and mitochondrial biogenesis in kidney diseases. Biomolecules 2020;10.
28. Bouchez C, Devin A. Mitochondrial biogenesis and mitochondrial reactive oxygen species (ROS): A complex relationship regulated by the cAMP/PKA signaling pathway. Cells 2019;8.
29. Chen N, Ge MM, Li DY, Wang XM, Liu DQ, Ye DW, et al. beta2-adrenoreceptor agonist ameliorates mechanical allodynia in paclitaxel-induced neuropathic pain via induction of mitochondrial biogenesis. Biomed Pharmacother 2021;144:112331.
30. Ege E, Briggi D, Vu P, Cheng J, Lin F, Xu J. Targeting dorsal root ganglia for chemotherapy-induced peripheral neuropathy: from bench to bedside. Ther Adv Neurol Disord 2024;17:17562864241252718.

31. Eldridge S, Guo L, Hamre J, 3rd. A comparative review of chemotherapy-induced peripheral neuropathy in in vivo and in vitro models. Toxicol Pathol 2020;48:190-201.
32. Pozzi E, Terribile G, Cherchi L, Di Girolamo S, Sancini G, Alberti P. Ion channel and transporter involvement in chemotherapy-induced peripheral neurotoxicity. Int J Mol Sci 2024;25.
33. Chen X, Gan Y, Au NPB, Ma CHE. Current understanding of the molecular mechanisms of chemotherapy-induced peripheral neuropathy. Front Mol Neurosci 2024;17:1345811.
34. Latremoliere A, Woolf CJ. Central sensitization: A generator of pain hypersensitivity by central neural plasticity. J Pain 2009;10:895-926.
35. Gao X, Kim HK, Mo Chung J, Chung K. Reactive oxygen species (ROS) are involved in enhancement of NMDA-receptor phosphorylation in animal models of pain. Pain 2007;131:262-71.
36. Shim HS, Bae C, Wang J, Lee KH, Hankerd KM, Kim HK, et al. Peripheral and central oxidative stress in chemotherapy-induced neuropathic pain. Mol Pain 2019;15:1744806919840098.
37. Bae C, Wang J, Shim HS, Tang SJ, Chung JM, La JH. Mitochondrial superoxide increases excitatory synaptic strength in spinal dorsal horn neurons of neuropathic mice. Mol Pain 2018;14:1744806918797032.
38. Schwartz ES, Kim HY, Wang J, Lee I, Klann E, Chung JM, et al. Persistent pain is dependent on spinal mitochondrial antioxidant levels. J Neurosci 2009;29:159-68.
39. Maher P, Schubert D. Signaling by reactive oxygen species in the nervous system. Cell Mol Life Sci 2000;57:1287-305.
40. Al-Kuraishy HM, Al-Gareeb AI, Naji MT, Al-Mamorry F. Role of vinpocetine in ischemic stroke and poststroke outcomes: A critical review. Brain Circ 2020;6:1-10.
41. Sheng J, Zhang S, Wu L, Kumar G, Liao Y, Gk P, et al. Inhibition of phosphodiesterase: A novel therapeutic target for the treatment of mild cognitive impairment and Alzheimer's disease. Front Aging Neurosci 2022;14:1019187.
42. Pereira C, Agostinho P, Moreira PI, Duarte AI, Santos MS, Oliveira CR. Neuroprotection strategies: effect of vinpocetine in vitro oxidative stress models. Acta Med Port 2003;16:401-6.
43. Bagri K, Deshmukh R. Vinpocetine restores cognitive and motor functions in traumatic brain injury challenged rats. Inflammopharmacology 2022;30:2243-59.
44. Lourenco-Gonzalez Y, Fattori V, Domiciano TP, Rossaneis AC, Borghi SM, Zaninelli TH, et al. Repurposing of the nootropic drug vinpocetine as an analgesic and anti-inflammatory agent: Evidence in a mouse model of superoxide anion-triggered inflammation. Mediators Inflamm 2019;2019:6481812.
45. Abdel Salam OM. Vinpocetine and piracetam exert antinociceptive effect in visceral pain model in mice. Pharmacol Rep 2006;58:680-91.
46. Toma W, Kyte SL, Bagdas D, Alkhlaif Y, Alsharari SD, Lichtman AH, et al. Effects of paclitaxel on the development of neuropathy and affective behaviors in the mouse. Neuropharmacology 2017;117:305-15.

47. Kim L, Nan G, Kim HY, Cha M, Lee BH. Modulation of chemotherapy-induced peripheral neuropathy by JZL195 through glia and the endocannabinoid system. Biomed Pharmacother 2024;180:117515.
48. Chaplan SR, Bach FW, Pogrel JW, Chung JM, Yaksh TL. Quantitative assessment of tactile allodynia in the rat paw. J Neurosci Methods 1994;53:55-63.
49. Kim MJ, Hong BH, Zhang EJ, Ko YK, Lee WH. Antinociceptive effects of intraperitoneal and intrathecal vitamin e in the rat formalin test. Korean J Pain 2012;25:238-44.
50. Stanford KR, Hadley SH, Barannikov I, Ajmo JM, Bahia PK, Taylor-Clark TE. Antimycin A-induced mitochondrial dysfunction activates vagal sensory neurons via ROS-dependent activation of TRPA1 and ROS-independent activation of TRPV1. Brain Res 2019;1715:94-105.
51. Kim HY, Chung JM, Chung K. Increased production of mitochondrial superoxide in the spinal cord induces pain behaviors in mice: The effect of mitochondrial electron transport complex inhibitors. Neurosci Lett 2008;447:87-91.
52. Griffiths LA, Flatters SJ. Pharmacological modulation of the mitochondrial electron transport chain in paclitaxel-induced painful peripheral neuropathy. J Pain 2015;16:981-94.
53. La JH, Wang J, Bittar A, Shim HS, Bae C, Chung JM. Differential involvement of reactive oxygen species in a mouse model of capsaicin-induced secondary mechanical hyperalgesia and allodynia. Mol Pain 2017;13:1744806917713907.
54. You W, Knoops K, Berendschot T, Benedikter BJ, Webers CAB, Reutelingsperger CPM, et al. PGC-1a mediated mitochondrial biogenesis promotes recovery and survival of neuronal cells from cellular degeneration. Cell Death Discov 2024;10:180.
55. Zong Y, Li H, Liao P, Chen L, Pan Y, Zheng Y, et al. Mitochondrial dysfunction: mechanisms and advances in therapy. Signal Transduct Target Ther 2024;9:124.
56. Jiang J, Parameshwaran K, Seibenhener ML, Kang MG, Suppiramaniam V, Huganir RL, et al. AMPA receptor trafficking and synaptic plasticity require SQSTM1/p62. Hippocampus 2009;19:392-406.
57. Esteban JA, Shi SH, Wilson C, Nuriya M, Huganir RL, Malinow R. PKA phosphorylation of AMPA receptor subunits controls synaptic trafficking underlying plasticity. Nat Neurosci 2003;6:136-43.
58. Han Y, Smith MT. Pathobiology of cancer chemotherapy-induced peripheral neuropathy (CIPN). Front Pharmacol 2013;4:156.
59. Wang M, Cheng HL, Lopez V, Sundar R, Yorke J, Molassiotis A. Redefining chemotherapy-induced peripheral neuropathy through symptom cluster analysis and patient-reported outcome data over time. BMC Cancer 2019;19:1151.
60. Avallone A, Bimonte S, Cardone C, Cascella M, Cuomo A. Pathophysiology and therapeutic perspectives for chemotherapy-induced peripheral neuropathy. Anticancer Res 2022;42:4667-78.
61. Bacalhau C, Costa-Pereira JT, Tavares I. Preclinical research in paclitaxel-induced neuropathic pain: a systematic review. Front Vet Sci 2023;10:1264668.

62. Klein I, Lehmann HC. Pathomechanisms of paclitaxel-induced peripheral neuropathy. Toxics 2021;9:229.
63. Areti A, Yerra VG, Naidu VGM, Kumar A. Oxidative stress and nerve damage: Role in chemotherapy induced peripheral neuropathy. Redox Biol. 2014;2:289-95.
64. Araldi D, Khomula EV, Bonet IJM, Bogen O, Green PG, Levine JD. Role of pattern recognition receptors in chemotherapy-induced neuropathic pain. Brain 2024;147:1025-42.
65. Finnerup NB, Kuner R, Jensen TS. Neuropathic pain: From mechanisms to treatment. Physiol Rev 2021;101:259-301.
66. Colvin LA. Chemotherapy-induced peripheral neuropathy: where are we now? Pain 2019;160 Suppl 1:S1-s10.
67. Carrasco C, Naziroğlu M, Rodríguez AB, Pariente JA. Neuropathic pain: Delving into the oxidative origin and the possible implication of transient receptor potential channels. Front Physiol 2018;9:95.
68. Maioli NA, Zarpelon A, Mizokami S, Calixto-Campos C, Guazelli CFS, Hohmann MSN, et al. The superoxide anion donor, potassium superoxide, induces pain and inflammation in mice through production of reactive oxygen species and cyclooxygenase-2. Braz J Med Biol Res. 2015;0.
69. Shekarian M, Salehi I, Raoufi S, Asadbegi M, Kourosh-Arami M, Komaki A. Neuroprotective effects of vinpocetine, as a phosphodiesterase 1 inhibitor, on long-term potentiation in a rat model of Alzheimer's disease. BMC Neurosci 2023;24:20.
70. Deshmukh R, Sharma V, Mehan S, Sharma N, Bedi KL. Amelioration of intracerebroventricular streptozotocin induced cognitive dysfunction and oxidative stress by vinpocetine - a PDE1 inhibitor. Eur J Pharmacol 2009;620:49-56.
71. Chen X, Guo C, Kong J. Oxidative stress in neurodegenerative diseases. Neural Regen Res 2012;7:376-85.
72. Cenini G, Lloret A, Cascella R. Oxidative stress in neurodegenerative diseases: From a mitochondrial point of view. Oxid Med Cell Longev 2019;2019:2105607.
73. Zhao M, Zhang X, Tao X, Zhang B, Sun C, Wang P, et al. Sirt2 in the spinal cord regulates chronic neuropathic pain through Nrf2-mediated oxidative stress pathway in rats. Front Pharmacol 2021;12:646477.
74. Yowtak J, Lee KY, Kim HY, Wang J, Kim HK, Chung K, et al. Reactive oxygen species contribute to neuropathic pain by reducing spinal GABA release. Pain 2011;152:844-52.
75. Li S, Li X, Xie X, Wei X, Yu C, Cheung CW, et al. N-Acetylcysteine attenuates hyperalgesia in rats with diabetic neuropathic pain: Role of oxidative stress and inflammatory mediators and CXCR4. J Diabetes Res. 2021;2021:8862910.
76. Doyle TM, Salvemini D. Mini-Review: Mitochondrial dysfunction and chemotherapy-induced neuropathic pain. Neurosci Lett 2021;760:136087.
77. Flynn JM, Melov S. SOD2 in mitochondrial dysfunction and neurodegeneration. Free Radic Biol Med 2013;62:4-12.
78. Miao L, St Clair DK. Regulation of superoxide dismutase genes: implications in disease. Free Radic Biol Med 2009;47:344-56.

79. Candas D, Li JJ. MnSOD in oxidative stress response-potential regulation via mitochondrial protein influx. Antioxid Redox Signal 2014;20:1599-617.
80. He J, Liu X, Su C, Wu F, Sun J, Zhang J, et al. Inhibition of mitochondrial oxidative damage improves reendothelialization capacity of endothelial progenitor cells via SIRT3 (Sirtuin 3)-enhanced SOD2 (Superoxide dismutase 2) deacetylation in hypertension. Arterioscler Thromb Vasc Biol. 2019;39:1682-98.
81. Yang S, Lian G. ROS and diseases: role in metabolism and energy supply. Mol Cell Biochem 2020;467:1-12.
82. Qian L, Zhu Y, Deng C, Liang Z, Chen J, Chen Y, et al. Peroxisome proliferator-activated receptor gamma coactivator-1 (PGC-1) family in physiological and pathophysiological process and diseases. Signal Transduct Target Ther 2024;9:50.
83. Rius-Pérez S, Torres-Cuevas I, Millán I, Ortega Á L, Pérez S. PGC-1α, inflammation, and oxidative stress: An integrative view in metabolism. Oxid Med Cell Longev 2020;2020:1452696.
84. Carlson GC, Coulter DA. In vitro functional imaging in brain slices using fast voltage-sensitive dye imaging combined with whole-cell patch recording. Nat Protoc 2008;3:249-55.
85. Wang Y, Wu J, Wu Z, Lin Q, Yue Y, Fang L. Regulation of AMPA receptors in spinal nociception. Mol Pain 2010;6:5.
86. Kopach O, Voitenko N. Spinal AMPA receptors: Amenable players in central sensitization for chronic pain therapy? Channels (Austin) 2021;15:284-97.
87. Zhou X, Dong XW, Crona J, Maguire M, Priestley T. Vinpocetine is a potent blocker of rat NaV1.8 tetrodotoxin-resistant sodium channels. J Pharmacol Exp Ther 2003;306:498-504.
88. Li XH, Miao HH, Zhuo M. NMDA receptor dependent long-term potentiation in chronic pain. Neurochem Res 2019;44:531-8.
89. Teixeira-Santos L, Albino-Teixeira A, Pinho D. Neuroinflammation, oxidative stress and their interplay in neuropathic pain: Focus on specialized pro-resolving mediators and NADPH oxidase inhibitors as potential therapeutic strategies. Pharmacol Res 2020;162:105280.
90. Li B, Yu K, Zhou X, Sun J, Qi L, Li W, et al. Increased TSPO alleviates neuropathic pain by preventing pyroptosis via the AMPK-PGC-1α pathway. J Headache Pain 2025;26:16.
91. Jeon KI, Xu X, Aizawa T, Lim JH, Jono H, Kwon DS, et al. Vinpocetine inhibits NF-kappaB-dependent inflammation via an IKK-dependent but PDE-independent mechanism. Proc Natl Acad Sci U S A 2010;107:9795-800.
92. Kopach O, Viatchenko-Karpinski V, Atianjoh FE, Belan P, Tao YX, Voitenko N. PKCα is required for inflammation-induced trafficking of extrasynaptic AMPA receptors in tonically firing lamina II dorsal horn neurons during the maintenance of persistent inflammatory pain. J Pain 2013;14:182-92.
93. He Y, Wang ZJ. Spinal and afferent PKC signaling mechanisms that mediate chronic pain in sickle cell disease. Neurosci Lett 2019;706:56-60.

Abstract in Korean

항암화학요법으로 유발된 말초신경병증 동물 모델에서 vinpocetine의 통증 완화 기전 규명

항암화학요법으로 유발된 말초신경병증(chemotherapy-induced peripheral neuropathy, CIPN)은 항암 치료 과정에서 감각 이상, 만성 통증 및 운동 기능 장애를 유발하는 주요 부작용 중 하나이다. CIPN은 높은 유병률에도 불구하고 질병 기전이 복잡하고 다요인적인 특성을 가지므로, 효과적인 치료법이 제한적이다. 특히, 산화 스트레스(oxidative stress)와 미토콘드리아 기능 장애는 신경 손상과 통증 과민화의 주요 원인으로 작용한다. 과도한 활성산소(reactive oxygen species, ROS) 생성, 미토콘드리아 기능 저하 및 항산화 방어 기전의 손상은 CIPN의 진행을 촉진하며, 이에 따라 미토콘드리아는 중요한 치료 표적으로 주목받고 있다.

빈포세틴(vinpocetine)은 빈카민(vincamine)의 합성 유도체로, 항산화, 항염증 및 미토콘드리아 보호 효과를 보이며 신경 보호 작용을 나타낸다. 이러한 특성으로 인해 뇌졸중 및 치매와 같은 신경계 질환에서 널리 활용되고 있으나, CIPN에서의 역할은 아직 명확히 규명되지 않았다. 본 연구에서는 CIPN 모델에서 빈포세틴의 진통 효과 및 그 기전을 규명하고자 하였다.

CIPN을 유도하기 위해 마우스에 파클리탁셀(paclitaxel)을 투여한 후, 빈포세틴을 1회 또는 반복 투여하였다. 이후 기계적 통각과민(mechanical hypersensitivity), 열통각과민(thermal hypersensitivity), 냉통각과민(cold hypersensitivity)을 평가하기 위해 행동 실험을 수행하였다. 미토콘드리아 기능과 관련된 기전을 분석하기 위해 웨스턴 블롯(Western blot)을 이용하여 PGC-1α/NRF1/TFAM 경로 및 SOD2 발현 수준을 측정하였으며 MitoSOX 염색을 통해 미토콘드리아 내 ROS 수준을 평가하였다. 또한, 척수 신경 활성 변화를 평가하기 위해 전압 감수성 염색 영상(voltage-sensitive dye imaging, VSDI)을 적용하였다. AMPA, NMDA 수용체(NR2A, NR2B) 및 관련 키나아제(PKC-α,

CaMKII-α, PKA)의 발현 변화를 웨스턴 블롯을 통해 조사하였으며, 면역조직화학법을 이용하여 척수 후각(spinal cord dorsal horn)에서 AMPA 및 PKC-α의 발현 강도와 NeuN과의 공동 발현(colocalization)을 분석하였다.

연구 결과, 빈포세틴은 산화 스트레스로 유발된 통증을 효과적으로 감소시키는 것으로 나타났다. 빈포세틴의 적절한 통증 완화 농도를 테스트한 결과, 20 mg/kg 용량에서 통증 증상이 유의미하게 완화되었으며, 반복 투여 시 누적적인 진통 효과가 확인되었다. 또한, 빈포세틴은 CIPN의 초기 및 후기 단계에서 척수 수준에서의 진통 효과를 보였다. 반복적인 빈포세틴 투여는 미토콘드리아 내 활성산소 생성을 감소시키고, PGC-1α/NRF1/TFAM 신호 경로를 활성화하며, SOD2 발현을 회복시켰다. VSDI 분석 결과, CIPN 모델에서 척수 후각 자극 시 대조군과 유의미한 차이를 보이는 임계값이 0.3 mA임을 확인하였다. 또한, VSDI 분석을 통해 빈포세틴 처리 후 신경 과흥분성이 감소하였으며, 그 효과가 2시간 이상 지속됨을 확인하였다. 반복적인 빈포세틴 투여 후 AMPA 및 NR2B 수용체의 발현 감소와 PKC-α 억제는 중추 감작(central sensitization) 감소를 시사하였다. 면역조직화학 분석을 통해 AMPA 및 PKC-α의 발현 강도가 감소하였으며, 척수 후각 뉴런과의 공동 발현 또한 줄어든 것을 확인하였다.

본 연구는 빈포세틴이 미토콘드리아 보호 및 중추 감작 조절을 통해 CIPN 치료의 유망한 후보 물질이 될 가능성이 있음을 시사한다. 또한, 빈포세틴은 미토콘드리아 항상성을 회복하고, 산화 스트레스를 감소시키며, 신경 흥분성을 조절함으로써 CIPN 관리에 효과적인 전략이 될 수 있다.

핵심되는 말: 화학요법 유발 말초신경병증, 빈포세틴, 미토콘드리아 생합성, 산화 스트레스, 신경 과흥분성, 중추 감작